ENCLOSURE 8

TN Calculation NUH32PHB-0212, CCNPP-FC Transfer Cask Structural Evaluation – Accident Conditions, 75G Side Drop and 75G Top End Drop Cases

AREVA TRANSNUCLEAR INC.	Form 3.2-1 Calculation Cover Sheet TIP 3.2 (Revision 5)	Calculation No.: NUH32PHB-0212
		Revision No.: 1
		Page1 of 60

DCR NO (if applicable) : NUH32PHB-009	PROJECT NAME: NUHOMS® 32PHB System
PROJECT NO: 10955	CLIENT: CENG - Calvert Cliff Nuclear Power Plant (CCNPP)

CALCULATION TITLE:

CCNPP-FC Transfer Cask Structural Evaluation – Accident Conditions, 75G Side Drop and 75G Top End Drop Cases.

SUMMARY DESCRIPTION:

1) Calculation Summary

The Calvert Cliffs Nuclear Power Plant Transfer Cask (CCNPP-FC TC), part of the NUHOMS® 32PHB System for Storage, constitutes a minor modification of the licensed design of CCNPP transfer cask (NUHOMS® 32P system). The design modification consists of the new top cover plate design with vent openings around the plate periphery and added spacer disk mounted to bottom cover plate that allow for forced convection cooling of cask interior.

The calculation documents results of the new design stress evaluation for accident conditions, for two accident scenarios: 75G Side Drop and 75G Top End Drop.

2) Storage Media Description

Secure network server initially, then redundant tape backup (Same as Rev. 0)

If original issue, is licensing review per TIP 3.5 required? N/A

Yes ☐ **No** ☐ **(explain below)** **Licensing Review No.:** ____________________

Software Utilized (subject to test requirements of TIP 3.3):	Version:
ANSYS	10A1

Calculation is complete: Originator Name and Signature: Huan Li [signature]	Date: 11/9/10
Calculation has been checked for consistency, completeness and correctness: Checker Name and Signature: Raheel Haroon [signature]	Date: 11/9/10
Calculation is approved for use: Project Engineer Name and Signature: Kamran Tavassoli [signature]	Date: 11/9/10

REVISION SUMMARY

REV.	DESCRIPTION OF CHANGES	AFFECTED PAGES	AFFECTED Computational I/O
0	Initial Issue	All	All
1	Update some of the references in the calculation	1,2,6,10	None

TABLE OF CONTENTS

LIST OF TABLES

Page

LIST OF FIGURES

1. Purpose

The CCNPP-FC transfer cask constitutes a minor modification of the licensed design of CCNPP transfer cask. The design modification consists of the new top cover plate design with vent openings around the plate periphery that vent out forced air that is injected at the bottom of the cask, and of the added spacer disk with wedge shaped protrusions mounted to the bottom cover plate to facilitate air flow coming through ram access opening to the annular space around the DSC.

Calculation documents results of CCNPP-FC on-site transfer cask stress evaluation for the design accident scenarios: 75G Side Drop and 75G Top End Drops. These two accident scenarios are deemed the most appropriate accident scenarios to conservatively assess modified stress magnitudes and patterns due to the new design of Top Cover Plate. The bounding 75G inertia load magnitude is chosen based on Ref. [3], Table 7.1 specification.

2. References

1. Transnuclear Calculation NUH32PHB-0201, Revision 0, "NUHOMS® 32PHB Weight Calculation of DSC/TC System."
2. ANSYS Release 10.0A1, UP20060501. Release 10 Documentation for ANSYS.
3. Transnuclear Document NUH32PHB.0101, Revision 2, "Design Criteria Document (DCD) for the NUHOMS® 32PHB System for Storage."
4. ASME Boiler and Pressure Vessel Code, Section III, Division 1, Subsection NC, 1992.
5. ASME Boiler and Pressure Vessel Code, Section II, Part D, 1992.
6. ASME Boiler and Pressure Vessel Code, Section III, Appendix F, 1992.
7. Transnuclear Calculation 1095-15 Revision 0, "NUHOMS 32P – Dynamic Stress Strain Lead Properties at Different Temperatures."
8. Machinery Handbook, Edition 24, Industrial Press, 1992.
9. Baumeister T. "Marks' Standard Handbook for Mechanical Engineers," Seventh Edition.
10. Warren C. Young, Richard G. Budynas, "Roark's Formulas for Stress and Strain," Seventh Edition, McGraw-Hill.
11. Gordon, J. L., "OUTCUR: An Automated Evaluation of Two-Dimensional Finite Element Stresses" according to ASME, Paper No. 76-WA/PVP-16, ASME Winter Annual Meeting (December 1976).
12. ORNL/M-5003, "Radioactive Materials Packaging Handbook, Design, Operations, and Maintenance," 1998.
13. Transnuclear Calculation NUH32PHB-0401, Rev. 0, "Transnuclear Calculation Thermal Evaluation of NUHOMS 32PHB Transfer Cask for Normal, Off Normal, and Accident Conditions (Steady State)."
14. Not used.
15. Transnuclear Calculation NUH32PHB-0211, Rev. 1, "Reconciliation for Transfer Cask CCNPP-FC Structural Evaluation."

3. ANSYS Run Documentation

(All runs use ANSYS Version 10.0 on Opteron Linux Platform)

Table 1 Files Used in Calculation

File ID	Description	Date / Time[(1)]
Input Model and Macro files		
nuh32phbcaskmod4.inp	input file for 3D model generation (stress analysis)	11/23/2009 20:38:54
nuh32phbcaskmod4lim.inp	input file for 3D model generation (limit analysis))	11/23/2009 20:38:54
nuh32phbcaskmod4.db	3D model database (stress analysis)	11/23/2009 21:29:27
nuh32phbcaskmod4lim.db	3D model database (stress analysis)	11/23/2009 21:29:07
agennuh32phbcaskmod4.macro	macro file used in generation of nuh32phbcaskmod4.db database file	11/23/2009 21:13:39
agennuh32phbcaskmod4lim.macro	macro file used in generation of nuh32phbcaskmod4lim.db database file	11/23/2009 21:15:16
arunnuh32phbcaskmod4[lim,sd].macro	macro files used in analysis runs	07/30/2009 23:11:01
postqnuh32phbcaskpathmod4.macro	macro file used in stress post-processing	10/12/2009 10:27:01
postqnuh32phbcaskpathmod4.inp	input file used in stress post-processing	10/12/2009 11:26:41
Horizontal Side Drop		
nuh32phbcaskmod4g75sd6.[ext] [ext]={inp;out;db;rst,macro}	75G side drop stress analysis	11/24/2009 01:29:54
nuh32phbcaskmod4limg120sd12.[ext] [ext]={inp;out;db;rst,macro}	Side Drop Collapse Limit Analysis	12/08/2009 07:04:49
Top End Drop		
nuh32phbcaskmod4top8.[ext] [ext]={inp;out;db;rst,macro}	75G Top End Drop Stress Analysis	11/24/2009 03:28:03

Note:Date & Time for main runs are from the listing at the end of the output files. For other files (e.g., .db files), dates & times are reported by the OS on the report issue date, these values may be changed by windows depending on time of the year (e.g., daylight savings time) and time zones.

4. Assumptions

1. For all accident cases, material properties of cask components are evaluated at temperature 400 °F. Stress criteria are evaluated at temperature of 400 °F. These temperatures constitute conservative estimation of anticipated temperature range [13].
2. The DSC structure impact is not modeled explicitly but simulated as a profiled contact pressure load. Load modeling details and assumptions are presented in 6.5.4. The use of contact pressure loads maximizes bending deformation of cask structure. In result, it is adding an additional conservatism in ASME code stress evaluations.
3. The weight of payload was conservatively enveloped by 96000 lb. The assumed value exceeds payload weight magnitude assessed in calculation [1].
4. The effect of outer shell assembly components is not modeled explicitly in the analysis. The impact of the weight of the major outer shell components (neutron shield, outer shell) encompassing structural shell component is accounted for by modeling 16000 lb surface weight distributed uniformly over the outer surface of structural shell. The assumed value exceeds outer shell assembly components weight magnitude assessed in calculation [1].
5. The effect of neutron shield assembly secured on top cover plate is not modeled explicitly in the analysis. The impact of the weight of the assembly is accounted for by modeling 1400 lb surface weight distributed over the outer surface of top cover plate. The assumed value exceeds neutron shell assembly components weight magnitude assessed in calculation [1].
6. The lead shielding is assumed to fill completely the lead cavity such that deformations of the inner shell immediately load the lead. Steel to lead interface contact is modeled assuming friction coefficient 0.25. This assumption is deemed the conservative approximation.
7. The impact properties of lead are modeled using stress-strain data, referring to strain rate of 100 in/in/sec. This strain rate value was assessed as the legitimate one for postulated drop conditions of transfer cask. Details of that assumption are discussed in Section 6.3.
8. RAM Access Cover Plate is not taken credit for. The assumption reduces conservatively the stiffness of the ram access penetration assembly and maximizes stresses in the RAM Access Penetration Ring.
9. The small longitudinal offset (≈0.1") of the Bottom End Plate (relative to the Bottom Support Ring forging) is not explicitly modeled. This modification required small adjustments in the geometry of the Ram Access Ring. However, the offset has been taken credit for in Bottom End Drop analysis through the specification of 0.1" gap distance between Bottom End Plate and impact surface. This model simplification is deemed not to affect results therefore.
10. The half-inch thick aluminum spacer disk, placed between DSC and bottom cover plate is not credited in the analysis. Modeling of this aluminum part is not needed when DSC load is modeled conservatively by means of uniform contact pressure.
11. The model assumes bolt hole diameter 1.88", instead of 1.92", in the Top Cover Plate. Such the difference is assessed insignificant for the results.
12. Detail assumptions referring to simulation cask drop events in the framework of static nonlinear elastic-plastic approach are delineated in Section 7.
13. Welds are not qualified in this calculation. Weld qualification for Service Level D conditions is addressed in Reference [15].

5. Stress Criteria

The CCNPP-FC on-site transfer cask is designed to meet the criteria of ASME Code Subsection NC for Class 2 components [3].

The acceptability of the design for Service Level D conditions is assessed by stress criteria stated in Reference [3]. The criteria are based on Appendix F, Section F-1341.2 (Plastic Analysis) of ASME code, or Appendix F, Section F-1341.3 (Limit Analysis Collapse Load) [6]. For accident conditions (Service Level D), the ASME code criteria are intended to affirm structural integrity of the design but to allow for the loss of operability of components during or after postulated accident. In particular, the bearing stresses need not to be evaluated except for pinned or bolted joints (F-1341.6).

The code imposes stress limits on

1. general primary membrane stress intensity (PM),
2. maximum primary stress intensity (PL, PL+PB),
3. average primary shear across a section loaded in pure shear.

The ASME code limits are 0.7^*S_u ($max(0.7S_u,S_y+(S_u-S_y)/3$ for austenitic steel, high nickel alloy steel, copper-nickel alloy steel) for general primary membrane stress intensity , 0.9^*S_u - for maximum primary stress intensity, and 0.42^*S_u for average primary shear. The first two criteria are determined to be bounding for this calculation and are used in the assessments. The third criterion applies only to special situations. It will be automatically satisfied when wall averaged stress intensities do not exceed 0.84^*S_u.

In lieu of above three stress criteria, cask design integrity can be assessed by means of limit analysis collapse load. Per F-1341.3 of ASME code, static load shall not exceed 90% of the limit analysis collapse load using a yield stress, which is the lesser of $2.3S_m$ and $0.7S_u$. In order to qualify design for 75G drop load, the limit analysis collapse load is required to exceed value 75G/0.9 = 83.3G. This criterion was employed in 75G side drop case to eliminate potential ambiguity in ASME code stress qualification of top cover component.

Per ASME code, the general primary stress PM is interpreted as an average stress across the solid section of structural component, must be controlled only by external loads, shall not account for local effects of geometric or material discontinuities and stress concentrations, and have to be produced only by pressure and/or mechanical loads.

The local membrane stress PL is the same as PM, except that it takes also into account the effect of gross discontinuities in locations where force redistribution may lead to excessive deformations. Primary bending stress PB is a variable part of stress across the solid section, must be controlled only by external loads; shall not account for the local effects of discontinuities and concentrations, and have to be produced only by pressure and/or mechanical loads.

Qualification sections comprise of all sections of the packaging structure that potentially can contribute to design collapse or excessive plastic deformation of the structure. For each component, ASME code stress classification is conducted for all shell and plate sections, and for all significant stress paths of more complicated geometrical shapes. Section 8.1 describes stress classification paths employed in stress screening evaluation.

Stress path data information and visual stress results, obtained for each component, were analyzed and compared against the applicable stress allowables.

Table 2 shows applicable acceptance criteria for cask steel components.

Table 2 Acceptance Criteria for Steel Components

Allowable Stresses	**SA-240 Type 304 Austenitic Stainless Steel Plate (18Cr - 8Ni)**				**SA-182 Type F304N Austenitic Stainless Steel Forgings (18Cr - 8Ni - N)**			
Temperature	Properties		Level D Allowables		Properties		Level D Allowables	
	S_y	20.7 ksi	PM	45.1 ksi	S_y	22.7 ksi	PM	51.2 ksi
400 °F	S_u	64.4 ksi	PL	58.0 ksi	S_u	73.2 ksi	PL	65.9 ksi
	S_m	18.7 ksi	PL+PB	58.0 ksi	S_m	20.3 ksi	PL+PB	65.9 ksi
Allowable Stresses	**SA-516 Type 70 Carbon Steel Plate**							
Temperature	Properties		Level D Allowables					
	S_y	32.6 ksi	PM	49.0 ksi				
400 °F	S_u	70.0 ksi	PL	63.0 ksi				
	S_m	21.7 ksi	PL+PB	63.0 ksi				

Per Reference [3], no weld strength limits are imposed on the cask design for Plastic Analysis, for Service Level D conditions.

The stress criteria for top cover plate bolts are [3]: average tension - $\min(S_y, 0.7S_u)$=87.5 ksi; tension plus bending - S_u = 125 ksi; average shear - $\min(0.6S_y, 0.42S_u)$ = 52.5 ksi, and interaction equation of Appendix F (F-1335.3) of ASME code.

The bounding 75G inertia load magnitude is chosen based on Ref. [3], Table 7.1 specification.

6. Model Description

6.1. Geometry

The schematic of structural components of the 3D model of NUH32PHB cask is presented in Figure 1. Additional plots of the model are presented in Section 10 (Figure 3 through Figure 5).

Materials of the design used in model specifications are documented in Section 6.3.

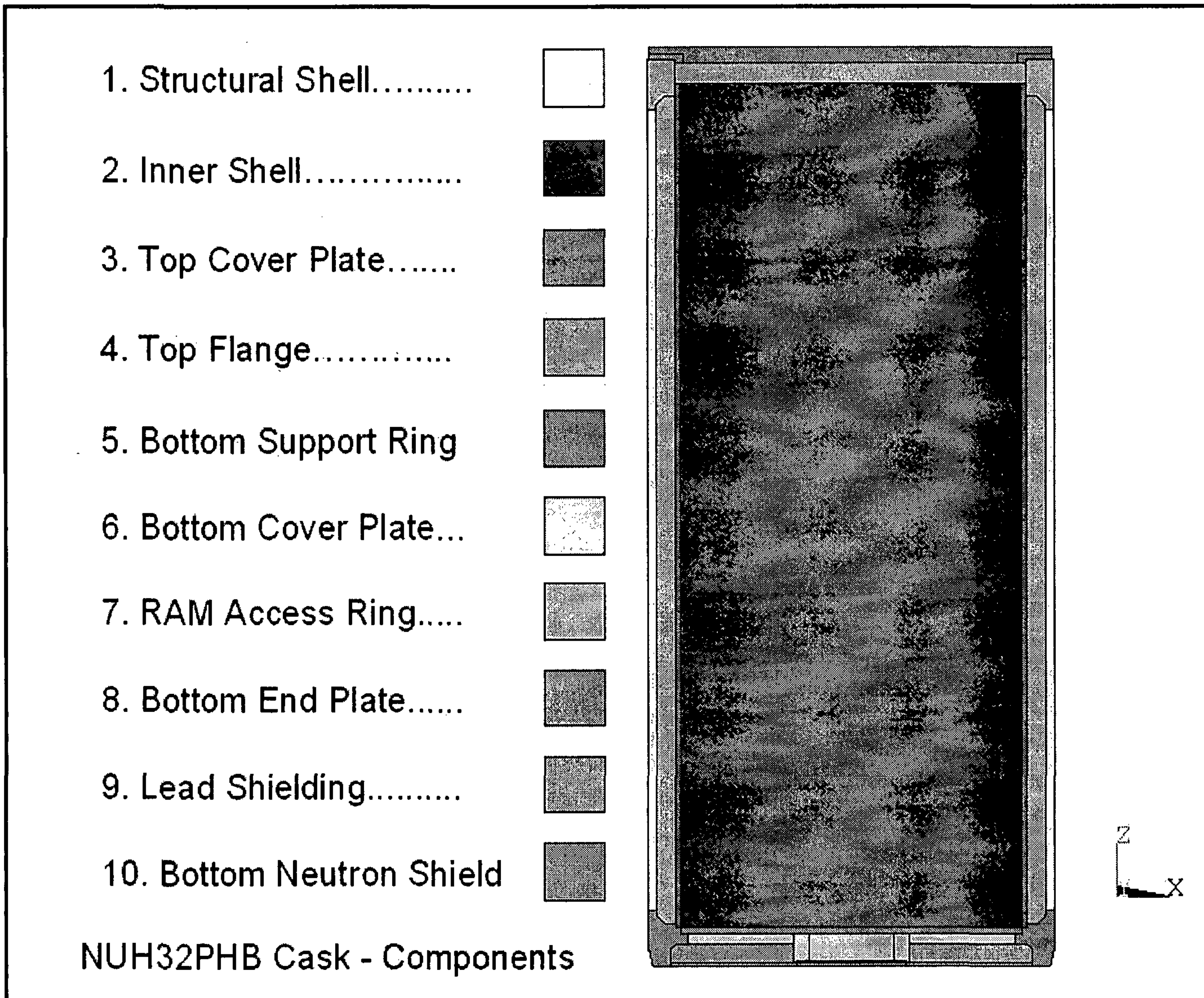

Figure 1 Schematic of the NUH32PHB Cask

The 3D FEA model is designed to represent 180-degree symmetry sector of cask body. The model is suitable to analyze cask assembly structure for 180° symmetry loads and boundary conditions.

The model represents NUH32PHB cask by ten structural components: Structural Shell, Inner Shell, Top Cover Plate, Top Flange, Bottom Support Ring, Bottom Cover Plate, Ram Access Ring, Bottom End Plate, Lead Shielding, and NS-3 Bottom Neutron Shield.

6.2. *Material Components*

The following structural components are evaluated in this calculation (TABLE 3):

TABLE 3 Material Components

#	Components	Material Specification
1	Structural Shell	SA-516 Type 70 Carbon Steel Plate
2	Inner Shell	SA-240 Type 304 Stainless Steel Plate
3	Top Cover Plate	SA-240 Type 304 Stainless Steel Plate
4	Top Flange	SA-182 Type F304N Stainless Steel Forging
5	Bottom Support Ring	SA-182 Type F304N Stainless Steel Forging
6	Bottom Cover Plate	SA-240 Type 304 Stainless Steel Plate
7	RAM Access Ring (1)	SA-182 Type F304N Stainless Steel Forging
8	Bottom End Plate	SA-240 Type 304 Stainless Steel Plate
9	Lead Shielding	ASTM B29 Chemical Copper Lead
10	Bottom Neutron Shielding	NS-3 Bisco Products Inc

Note 1: Reference [1] uses name RAM Access Penetration Ring for this Component.

6.3. *Material Properties*

Steel Plates Material

The following tables, Table 4 through Table 6, list stainless steel or carbon steel material properties available in the model material database. The material properties are based on ASME BPV Code, Section II, 1992 [5], pertinent for NUH32PHB cask stress evaluations [3].

Table 4 Material Properties of Stainless Steel SA 240 Type 304

Stainless Steel SA 240 Type 304 (18cr-8ni) -ASME 1992									
Temperature	[°F]	0	70	200	300	400	500	600	700
Sy	[psi]	30000	30000	25000	22500	20700	19400	18200	17700
Su	[psi]	75000	75000	71000	66000	64400	63500	63500	63500
Sm	[psi]	20000	20000	20000	20000	18700	17500	16400	16000
E	[psi]	2.87E+07	2.83E+07	2.76E+07	2.70E+07	2.65E+07	2.58E+07	2.53E+07	2.48E+07

Table 5 Material Properties of Stainless Steel SA 182 Type F304N

Stainless Steel SA 182 Type F304N (18cr-8ni-n) ASME 1992									
Temperature	[°F]	0	70	200	300	400	500	600	700
Sy	[psi]	35000	35000	28700	25000	22500	20900	19800	19100
Su	[psi]	80000	80000	80000	75900	73200	71200	69700	68600
Sm	[psi]	23300	23300	23300	22500	20300	18800	17800	17200
E	[psi]	2.87E+07	2.83E+07	2.76E+07	2.70E+07	2.65E+07	2.58E+07	2.53E+07	2.48E+07

Table 6 Material Properties of Carbon Steel SA 516 Type 70

Carbon Steel SA516 Type 70 - ASME 1992									
Temperature	[°F]	0	70	200	300	400	500	600	700
Sy	[psi]	38000	38000	34600	33700	32600	30700	28100	27400
Su	[psi]	70000	70000	70000	70000	70000	70000	70000	70000
Sm	[psi]	23300	23300	23100	22500	21700	20500	18700	18300
E	[psi]	2.98E+07	2.95E+07	2.88E+07	2.83E+07	2.77E+07	2.73E+07	2.67E+07	2.55E+07

Poisson's ratio for steel components is 0.3; density is equal to 0.29 lb/in^3 (501.12 lb/ft^3).

Lead Material

Table 7 and Table 8, below, list lead material properties available in the model database. The properties are taken from Reference [3]. Dynamic properties, provided in the Table 8, were set up in Reference [7]. Reference [7] established the stress-strain relation presented in Table 8 for strain rate of 100 in/in/sec. This strain rate corresponds to dynamic impact velocity of dropping body about 50 ft/sec that envelops dynamic impact velocity of 30-foot drop of the cask [7, p. 1].

Table 7 Material Properties of Lead – Static Properties

Lead ASTM B29 - Chemical Lead - Static Properties								
Temperature	[°F]	70	100	175	250	325	440	620
E	[psi]	2.34E+06	2.30E+06	2.20E+06	2.09E+06	1.96E+06	1.74E+06	1.36E+06
S_y (**)	[psi]	512(*)	490	428	391	320	241(*)	110(*)

Notes: (*) Values obtained by an extrapolation; (**) Compression.

Table 8 Material Properties of Lead – Dynamic properties

Lead ASTM B29 - Chemical Lead - Dynamic Properties							
Temperature	[°F]	0	100	230	300	350	500
E	[psi]	1140/0.000485	1140/0.000485	1060/0.000485	1000/0.000485	970/0.000485	860/0.000485
Stress Strain Table							
Strain	[in/in]	0.000485	0.03	0.10	0.30	0.50	1.0
Stress @ 0 °F	[psi]	1140	2200	3300	4900	5600	5600
Stress @ 100 °F	[psi]	1140	2200	3300	4900	5600	5600
Stress @ 230 °F	[psi]	1060	2000	2800	3200	3600	3600
Stress @ 300 °F	[psi]	1000	1700	2380	2720	3060	3060
Stress @ 350 °F	[psi]	970	1500	2100	2400	2700	2700
Stress @ 500 °F	[psi]	860	1100	1260	1440	1620	1620

Poisson's ratio for lead is 0.45; density is equal to 710 lb/ft^3 [7].

Neutron Shield Material NS-3

The properties of neutron shielding material NS-3 are presented in Table 9. NS-3 material properties are taken from Reference 3. The density of 150 lb/ft^3 bounds conservatively values supplied in Reference [3].

Table 9 Mechanical Properties of Neutron Shielding Materials

Material Specification	Elastic modulus	Compressive Strength	Poisson's coefficient	Density
	(psi)	(psi)		lb/ft^3
NS-3	160000	3900	0.2	150

6.4. Material Models

6.4.1. Steel Plates

Steel material is modeled by means of bilinear kinematic hardening method (TB, BKIN). The material behavior is described by a bilinear total stress-total strain curve starting at the origin and with positive stress and strain values. The initial slope of the curve is taken as the elastic modulus of the material. At the specified yield stress, the curve continues along the second slope defined by the tangent modulus [2]. It is assumed that the tangent modulus amounts to 5% of elastic modulus.

6.4.2. Lead

Lead material is represented by the ANSYS multi-linear kinematic hardening material model (TB, KINH). The method belongs to family of multi-linear kinematic hardening models. The "total stress-total strain curve", is starting at the origin, with positive stress and strain values. The slope of the first segment of the curve corresponds to the elastic modulus of the material [2]. The slopes of the subsequent segments are derived from stress-strain data provided in Table 8.

6.5. Interfaces

6.5.1. Welds

The component interfaces in cask design include welded joints. Cask components and all its weld joints are under ASME code NC-Subsection jurisdiction [1]. Per ASME code requirement (Ref. [4], NC-3355), the cask component dimensions and shape of the edges shall be such as to permit complete fusion and complete joint penetration of weld grooves. Per NC-4245, complete joint penetration is considered to be accomplished when the acceptance criteria for examination specified in Subsection NC have been achieved.

Full penetration groove welds are designed and fabricated to transfer all loads (including bending) of part they are connecting. That is, if the base metal at weld location is shown to be qualified - then these welds are also qualified. All locations of full penetration welds are addressed in stress screening procedure described in Section 8. In consequence, this calculation does not require a separate evaluation of full penetration welded joints.

ASME code NC-Subsection requires partial penetration welds localized in an area of low stress.

Per Reference [3], for Service Level D conditions, weld qualification should to be addressed via elastic analysis methodology. Partial penetration welds are qualified via elastic analysis methodology in Reference [15].

6.5.2. Surface Contact

Boundaries between the steel and lead Gamma Shielding, between Top Cover Plate and the Top Flange, and between NS-3 Bottom Neutron Shielding and encasing it steel components are modeled with surface-to-surface contact elements CONTA173 and TARGE170.

Top Cover Plate interface (contact and target elements) is presented in Figure 6. Lead Shielding contact elements, and contact elements encasing NS-3 Bottom Neutron Shielding are presented in Figure 7 and Figure 8, respectively.

For Top Cover Plate and NS-3 Bottom Neutron Shielding closure interface no credit is taken for steel-to-steel friction (parameter MU=0). At Gamma Shielding component interface with encompassing steel, steel-to-lead friction factor MU=0.25.

6.5.3. Top Cover Plate Bolts

The Top Cover Plate bolt response to the imposed loads is modeled with nonlinear springs (COMBIN39) in tensile and shear directions. Because bolt holes in Top Cover Plate have been modeled explicitly, the top end nodes of bolt elements are coupled with Top Cover Plate interface be means of RBE3 ANSYS constraint equations. RBE3 constraint equations are allowing for more realistic modeling of shear interaction between bolts and plate interface by means of distributed forces/moments on nodes of top cover plate.

Spring specifications are based on bolt material and geometrical data summarized in Table 10, below.

Table 10 Lid Bolt Input Data [8], [9], [10]

BOLT MATERIAL		SA193 Gr B7		NUH32PHB
Top Cover Plate Bolts		1.75-5UNC-2A 5.5"LG		
MP197HB				
MATERIAL	SA193 Gr B7			
	1CR+0.2MO		@400 °F	
Su	125000 psi			
Sy [ksi]	91500 psi			
E	2.790E+07 psi			
bolt diameter	Db		1.75 in	
minimum diameter at shank	Dbh		1.75 in	
# of threads per inch	N		5.0	
Esmin - min pitch diameter	Esmin		1.6085 in	
minor diameter -conservative	Droot		1.4900 in	
diameter for tensile stress	Dba		1.5435 in	
bolt length	Lb		5.5	
cross sections	Aten		1.8712 in^2	
	Aroot		1.7437 in^2	
	Anom		2.4053 in^2	
cover thickness at bolt location	tbc		2.5000	
Effective length	Lbm	tbc+1/2*Db	3.375 in	
length of thread (Min)			4 in	
length in Plate			3.0000 in	

Note: Aten $=\pi*(Esmin/2-0.16238/N)^2$ (for Su>100 ksi), Aroot $=\pi/4*(Db-1.3/N)^2$ (conservative)

Axial Direction:

In the axial (tensile) direction, the springs are soft in compression since the bolts will carry no compressive loads (compression is carried by contacts between the top cover plate and the Top Flange). Tensile stiffness in the elastic range is as shown below in Table 11. After stress reaches yield, stiffness is reduced arbitrarily by a factor of 100 to account conservatively for softer bolt response in plastic range.

The evaluation worksheet of the spring specification is provided below in Table 11.

Transverse direction:

Shear stiffness is modeled in three parts: (1) initially, for displacements less than the radial clearance between the nominal bolt diameter and the bolt hole, the spring is soft. (2) Stiffness in the elastic range is then calculated as the stiffness of a shear beam. (3) After reaching shear yield, stiffness is reduced arbitrarily by 100.
The evaluation worksheet of spring specification for transverse (shear) directions is provided below in Table 12.

Table 11 Specification of COMBIN39 Elements in Tensile Direction

TENSILE DIRECTION				
Bolt yielding,Sy	@400 °F		9.150E+04	
$K_{axial}=A_{tensile}$*E/L=Aten*E/Lbm			1.547E+07 lb/in	
Tensile force at yielding				
	$F_y=S_y*A_{tensile}$		171219 lb	
displacement for yielding				
	$\delta=F_y/K_{axial}$		0.0111	
Tension - adjustment for final slope				
	x1=	0	f1	0
	x2=	0.0111	f2	171219
	x3=	1.0111	f3=f2+(x3-x2)*k3	
f3=f2+(x3-x2)*k3	k3=k2/100		f3=	325908
curve points specification		**tension with yielding**		

point #	δ	F
1	-1.0111	-1000
2	0	0
3	0.0111	171219
4	1.0111	325908

Table 12 Specification of COMBIN39 Elements in Shear Direction [10]

SHEAR DIRECTIONS (Roark's formulas …7Ed, Section 8.10)

deflection Ys due to shear load P:

Ys=F*(P*L/A*G)

F=10/9	(for cylindrical solid)	1.1111111		
G=E/(2*(1+NI))		1.07E+07		
$K_{shear}=P/Ys=A_{root}G/(FL)$		4.99E+06		
bolt hole		1.88		
bolt radial clearance		0.065		

low stiffnesss for radial displacements lesser than bolt clearance 0.065

curve points	δ	F
1	-1.065	-4.99E+06
2	-0.065	-1000
3	0	0
4	0.065	1000
5	1.065	4.99E+06

Bolt Shear Yielding

Assume	Sys=0.577*Sy	5.28E+04	psi
	Fys=Sys*Aroot	92057.5	
displacement for yielding	δ=Fys/Kshear	0.018450	in
total displacement for yielding	δys=gap +δ	0.0835	in

Shear- adjustment for final slope

F=Kshear*x	k2=Kshear			4.99E+06
	x1	0.065	f1=1000	1000
	x2	0.0835	f2=f1+(x2-x1)*k2	
	x3	1.0835	f3=f2+(x3-x2)*k3	
f2=f1+(x2-x1)*k2	k2=Kshear		f2=	93058
f3=f2+(x3-x2)*k3	k3=k2/100		f3=	142953

curve points specification **shear with yielding**

point #	δ	F
1	-1.0835	-142953
2	-0.0835	-93058
3	-0.0650	-1000
4	0.0000	0
5	0.0650	1000
6	0.0835	93058
7	1.0835	142953

6.5.4. Loads

Weight Load

The mass of components modeled and total mass of the package are presented in Table 13 below. Outer castable NS-3 neutron shield (located outside of cask shell) and top castable NS-3 neutron shield (located outside of top cover plate) are not included in the model. Because these components contribute noticeably to the overall mass of the cask, the masses of these components are conservatively estimated as 16000 lb (outer shield) and 1400 lb (top end shield and modeled as surface masses.

Table 13 Mass of Cask Components

COMPONENT	ELEMENT TYPE NUMBER	MATERIAL TYPE NUMBER	INPUT DENSITY	COMPONENT MASS
			[lb/in3]	[lb]
Structural Shell	1	1	0.29000	9369
Inner Shell	2	2	0.29000	3950
Top Cover Plate	3	3	0.29000	1938
Top Flange	4	4	0.29000	1542
Bottom Support Ring	5	5	0.29000	1765
Bottom Cover Plate	6	6	0.29000	841
RAM Access Ring	7	7	0.29000	147
Bottom End Plate	8	8	0.29000	403
Lead Shielding	18	18	0.41088	30671
Bottom Neutron Shielding	19	19	0.086806	570
Side Neutron Shield Assembly	14	14	3.8829	8000
Top Neutron Shield Assembly	21	21	3.7684	700
Cask Weight (Half Symmetry Model)				59896
Cask Weight (Total)				119792
Payload				96000
Total Weight of Package Analyzed				215792

DSC Load

DSC impact is applied to cask model based on the assumption of DSC weight of 96 kips. This value of DSC weight envelops DSC weight value calculated in Reference [1]. The DSC structure impact is not modeled explicitly but simulated as a profiled contact pressure load.

In case of side drop accident simulation the load is imposed as a pressure load distributed uniformly in axial direction over the effective length of inner shell and as the cosine shaped function in circumferential direction over the ±45° angle span (45° angle in 180-degree symmetry model). The specification of cosine shape function is provided in the section below.

In the case of top end drop the contact pressure load is defined as distributed uniformly over the contact area of DSC top end area with cask body.

Cosine Distributed Pressure Loading

The circumferential cosine distribution of pressure over a pressure load half angle, θ_{max}, is calculated as follows:

$$P_i = P_{\max} \cos(\pi\theta_i / 2\theta_{max})$$

where:

P_i = Pressure load at the angle θ_i.

$P_{\max}$ = Peak pressure load, at the base of the interface (θ_i=0).

θ_i = Circumferential angle corresponding to location of interest.

The circumferential distribution of pressure is illustrated in following sketch:

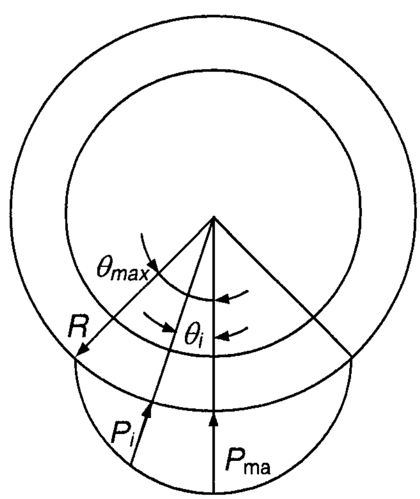

Figure 2 Circumferential Cosine Pressure Load Distribution

The peak pressure load, $P_{\max}$, can be determined by setting the integral of the vertical pressure components, Q_i, equal to the net force in transverse direction, F_t:

$$F_t = (\text{Transverse Component of G-load}) \times (\text{Imposed Weight Load}) = G_t \times W$$

as follows:

$$G_t \times W = F_t = \int_{-\theta_{max}}^{\theta_{max}} Q_i LR d\theta_i = \int_{-\theta_{max}}^{\theta_{max}} P_i \cos(\theta_i) LR d\theta_i = \int_{-\theta_{max}}^{\theta_{max}} P_{max} \cos\left(\frac{\pi\theta_i}{2\theta_{max}}\right)\cos(\theta_i) LR d\theta_i$$

$$= \frac{P_{max}LR}{2}\int_{-\theta_{max}}^{\theta_{max}}\left[\cos\left(\frac{\pi\theta_i}{2\theta_{max}}+\theta_i\right)+\cos\left(\frac{\pi\theta_i}{2\theta_{max}}-\theta_i\right)\right]d\theta_i = P_{max}LR\left[\frac{\sin\left(\frac{\pi}{2}+\theta_{max}\right)}{\left(\frac{\pi}{2\theta_{max}}\right)+1}+\frac{\sin\left(\frac{\pi}{2}-\theta_{max}\right)}{\left(\frac{\pi}{2\theta_{max}}\right)-1}\right]$$

In above formulas:

θ_i = Position angle of circumferential distribution

$\pm\theta_{max}$ = Circumferential span of pressure load

F_t = Net force in the transverse direction

L = Axial span of pressure load

R = Radius of pressure load surface

G_t = Acceleration in the transverse direction of cask

Rearranging terms gives the peak pressure, P_{max}, as follows:

$$P_{max} = \frac{G_t \times W}{L \times R}\left[\frac{\sin\left(\frac{\pi}{2}+\theta_{max}\right)}{\left(\frac{\pi}{2\theta_{max}}\right)+1}+\frac{\sin\left(\frac{\pi}{2}-\theta_{max}\right)}{\left(\frac{\pi}{2\theta_{max}}\right)-1}\right]^{-1}$$

Therefore, the pressure at any circumferential location is given by:

$$P_i = \frac{G_t \times W}{L \times R}\left[\frac{\sin\left(\frac{\pi}{2}+\theta_{max}\right)}{\left(\frac{\pi}{2\theta_{max}}\right)+1}+\frac{\sin\left(\frac{\pi}{2}-\theta_{max}\right)}{\left(\frac{\pi}{2\theta_{max}}\right)-1}\right]^{-1}\cos\left(\frac{\pi\theta_i}{2\theta_{max}}\right)$$

For example, the internal pressure due to payload applied for the 75G Side Drop case, distributed over ±45° angle circumferentially, with axial span 168.25 inch and inner shell radius 34.0 inch can be calculated as follows:

$$P_i = \frac{75 \times 96000}{168.25 \times 34.0} \times \frac{1}{\dfrac{\sin(90+45)}{(\dfrac{180}{2 \times 45})+1} + \dfrac{\sin(90-45)}{(\dfrac{180}{2 \times 45})-1}} \times \cos(\frac{180 \times 0}{2 \times 45}) = 1335\text{psi}$$

Pressure value calculated above is the peak pressure load P_{max} at interface base (circumferential angle 0°). Magnitudes of peak pressure P_{max} are calculated by ANSYS.

6.5.5. ANSYS Model Specifications

Table 14 shows ANSYS element types used to represent in analyses structural components of cask design.

Table 14 ANSYS Elements Specifications

COMPONENT	MATERIAL TYPE NUMBER	ELEMENT TYPE NUMBER	3D MODEL ELEMENTS
Outer Shell.	1	1	SOLID45
Inner Shell	2	2	SOLID45
Lid	3	3	SOLID45
Top Flange	4	4	SOLID45
Bottom Flange	5	5	SOLID45
Bottom Plate	6	6	SOLID45
RAM Access Ring	7	7	SOLID45
Bottom End Plate	8	8	SOLID45
Top Cover Plate Bolts (Radial Shear Interaction)	9	391	COMBIN39
Top Cover Plate Bolts (Tangential Shear Interaction)	9	392	COMBIN39
Top Cover Plate Bolts (Axial Interaction)	9	393	COMBIN39
Outer Neutron Shield Assembly	14	14	SURF154
Gamma Shield	18	18	SOLID45
Bottom Neutron Shield	19	19	SOLID45
Top Neutron Shield Assembly	21	21	SURF154
RBE3 Sustaining Element	99	99	MASS21

Table 15 shows specification of the contact interfaces between material components done by means of surface contact elements (elements CONTA173, TARGE170).

Table 15 ANSYS Elements Specifications – Contact elements

Contact Interface Description	Target Element Type Number	Contact Element Type Number.	Element Real Constant Number	Material Type Number
Top Cover Plate and Top Flange Chamfer Interface (Figure 6)	1101-1108	101-108	101-108	11
Top Cover Plate and Top Flange Interface Clamping Interface (Figure 6)	1111-1118	111-118	111-118	11
Bottom Neutron Shield Encasing Surface (Figure 8)	1121	121	121	12
Bottom Cover Plate to RAM Access Ring (between grove welds)	1131	131	131	20
Lead Shielding Contact Surface (Figure 7)	1201-1210	201-210	201-280	13

6.5.6. Boundary Conditions

The model was adapted to represent 180-degree part of cask structure with symmetrical boundary conditions.

Supplementary boundary conditions refer to specific load case scenario. In the case of 75G side drop cask structural shell is fixed for a small arc 15° (180-degree model) in circumferential direction to simulate semi-rigid impact conditions and minimal boundary conditions in z direction are applied to avoid rigid body motion of model. Boundary conditions for side drop case are illustrated in Figure 9.

In case of 75G Top End Drop analyses, the cask model is fixed minimally in lateral direction to avoid rigid body motion of model, while contact with impact surface is simulated by means surface contact elements with fixed rigid impact target plane.

7. Accidents Analyzed

7.1. 75G Side Drop

The weight of the DSC is imposed as a pressure load distributed uniformly in axial direction over the effective longitudinal span of inner shell and as the cosine shaped function in tangential direction over the ±45° angle span (45° angle in 180-degree symmetry model). The maximum of pressure is modeled at cask bottom (model symmetry line) is reaching 1335 psig at 75G inertia load.

The cosine distribution of contact pressure constitutes the standard, conservative approach used in side drop cask analyzes [12].

In the case of 75G side drop cask structural shell is fixed at the small 15° arc in circumferential direction to simulate semi-rigid impact conditions and minimal boundary conditions in z direction are applied to avoid rigid body motion of model. Such method of modeling of impact interface constitutes valid simulation semi-rigid interface of impact interface in static analyses.

The boundary conditions and DSC load distribution are shown in Figure 9 and Figure 10.

7.2. 75G Top End Drop

The weight of DSC is imposed as a pressure load distributed uniformly on inner surface of Top Cover Plate. The area of inner surface amounts 3588.6 in^2 (taken from ANSYS model). In result pressure for 75G top end drop as 75×96000/3588.6 =2006.35 psig.

Top end drop impact interface is modeled by means of surface contact elements with rigid flat surface target. The boundary conditions and DSC load distribution are shown in Figure 11.

8. Stress Results

8.1. Stress Classification Paths

Per ASME code requirements, stress classification sections or lines (paths) should comprise all sections of the steel structure that potentially can contribute to the design failure.

The path locations are described in Table 16 and illustrated in Figure 27 through Figure 29.

In order to achieve an adequate amount of information regarding each category of ASME code primary or secondary stresses for all cask components, stress information is collected for a comprehensive, pre-structured set of stress classification lines (paths).

Table 16 Stress Paths

Component	Stress Paths
Structural Shell	Paths are defined using all nodal points on the inside shell surface (shell ID) to the corresponding point on the shell OD.
Inner Shell	Paths are defined using all nodal points on the inside shell surface (shell ID) to the corresponding point on the shell OD.
Top Cover Plate	Paths are defined using nodal points on the inside face of the plate to the corresponding point on the outside surface.
Top Flange	Paths are defined from nodes on the inner surface to the corresponding nodes on the outer surface of cylinder and cone segments of flange for all meaningful stress flow routes
Bottom Support Ring	Paths are defined from all nodes on the inner surface to the corresponding nodes on the outer surface of cylinder and cone segments of flange for all meaningful stress flow routes.
Bottom Cover Plate	Paths are defined using all nodal points on the inside face of the plate to the corresponding points on the outside surface.
Bottom End Plate	Paths are defined using all nodal points on the inside face of the plate to the corresponding points on the outside surface.
Ram Access Ring	Paths are defined from nodes on the inside surface to the corresponding nodes on the outer surface of the ring cylinder

For shell and plate sections of the cask structure, the ASME code stress classification paths are predefined at all section locations as the across the wall thickness paths, normal to the cylinder or plate section mid-plane.

For more complicated shapes of cask components, the stress paths are also defined for most surface-node-to-surface-node trajectories, across the wall thickness, in locations and orientations meaningful for anticipated stress flow routes.

Path locations include all structure sections expected to provide meaningful information about stress flow.

In specification of path locations, no consideration is taken to separate paths defined at structural discontinuities from paths remote from structural discontinuities. Therefore, the average stresses over wall thickness can potentially represent equally the general primary membrane, or local primary membrane stresses; or can have features of secondary stresses. All wall averaged stresses taken from such broad collection of paths are assessed against the general primary membrane stress (PM) – as primary screening criterion to secure conservatism of stress screening methodology. The complete description of applied stress screening methodology, based on collected information about path stresses, is provided below.

Identification and qualification of primary stresses for Top Cover Plate in the side drop event required a more refined and laborious approach. Stress data interpretation for the plate required additional sorting out of local bearing stresses and stresses induced by local discontinuities that do not represent the primary stress designation in the ASME code. The stress qualification procedure for Top Cover Plate is described in detail in Section 8.3.

8.2. Stress Qualification Method

Stress information collected at predefined paths and/or stress qualification procedure is based on the method employed in the ANSYS code. The method used in ANSYS is based on Gordon methodology [2], [11]. Stress result data are mapped onto a path by first interpolating individually stress components (σ_x, σ_y, σ_z, σ_{xy}, σ_{xz}, σ_{zx}) to the path. Then, stress averaging through the wall path and the linearization are done independently for all six stress components.

Principal membrane stresses and membrane stress intensities are derived from membrane parts of the individual stress components. Similarly, linearized principal stresses and linearized stress intensity at the path section surface are derived from linearized individual stress components of that surface.

In the case of elastic-plastic stress analysis, the stress path evaluation in ANSYS brings the information about the membrane stress for the path (classified conservatively as PM stress), as well as the maximum stress intensity (classified conservatively as the primary stress) for the classification path, derived from the path total (not linearized) stresses.

Conservatively no distinction is assumed between paths located at gross or local discontinuities and areas remote from these discontinuities, and all path averaged stresses (including general primary stress intensities, PM, and local primary stress intensities, PL) are classified conservatively and reported as PM stresses and assessed against PM stress allowable.

Stress path evaluation in ANSYS brings also an information about the maximum stress intensity at the classification paths (classified conservatively as the primary stress), derived from the total (not linearized) path stresses. These values of maximum stress intensity are assessed against maximum stress intensity allowables, (PL+PB), as well as reported conservatively as the upper bounds of primary local stresses PL (PB=0), and assessed against PL stress allowables. Such approach secures both, the conservatism of assessments, as well as the efficiency of stress qualification procedure.

In case when obtained stresses exceed conservative criteria, the detail examination of stresses and the qualification of stress category is initiated. In the last resort the limit load collapse analysis is performed and studied to ensure that overall failure due to plastic hinge does not occur.

8.3. Analysis of Results – Discussion

8.3.1. Summary of Results

Table 17 and Table 18 show primary stresses obtained by means of automated, conservative stress screening procedure described in Section 8.2. Table 17 shows stresses obtained for 75G Side Drop case, while Table 18 shows stress results for 75G Top End Drop case. Both tables compare obtained stresses against stress allowable values delineated in Section 5.

Table 17 Stress Results – 75G Side Drop Case

CCNPP FC Transfer Cask			Side Drop – 75G Load								
			Max Stress [ksi] Stress Ratio [%]			Allowable [ksi]			Material Properties [ksi]		
#	Component	Material Specification	PM	PL	PL+PB	PM	PL	PL+PB	Sy	Su	Sm
1	*Structural Shell*	SA-516 Type 70 Carbon Steel Plate	39.9 81.5%	51.2 81.2%	51.2 81.2%	49.0	63.0	63.0	32.6	70	21.7
2	Inner Shell	SA-240 Type 304 Stainless Steel Plate	42.0 93.1%	44.3 76.4%	44.3 76.4%	45.1	58.0	58.0	20.7	64.4	18.7
3	Top Cover Plate	SA-240 Type 304 Stainless Steel Plate	**35.3**(*) 78.3%	**45.4**(*) 78.3%	**47.9**(*) 82.6%	45.1	58.0	58.0	20.7	64.4	18.7
4	Top Flange	SA-182 Type F304N Stainless Steel Forging	36.5 71.2%	51.6 78.3%	51.6 78.3%	51.2	65.9	65.9	22.7	73.2	20.3
5	Bottom Support Ring	SA-182 Type F304N Stainless Steel Forging	41.0 80.1%	44.2 67.0%	44.2 67.0%	51.2	65.9	65.9	22.7	73.2	20.3
6	Bottom Cover Plate	SA-240 Type 304 Stainless Steel Plate	39.4 87.4%	45.1 77.8%	45.1 77.8%	45.1	58.0	58.0	20.7	64.4	18.7
7	RAM Access Ring	SA-182 Type F304N Stainless Steel Forging	29.0 56.6%	42.6 64.7%	42.6 64.7%	51.2	65.9	65.9	22.7	73.2	20.3
8	Bottom End Plate	SA-240 Type 304 Stainless Steel Plate	41.1 91.2%	53.4 92.1%	53.4 92.1%	45.1	58.0	58.0	20.7	64.4	18.7

Note (*): Stresses for Top Cover Plate are qualified individually based on the separate, detailed qualification of the path stress data that sorted out data that do not have mandatory characteristics of the ASME categories of primary stress. (See Section 8.3.2 for discussion of Top Cover Plate stress evaluation).

Table 18 Stress Results – 75G Top End Drop Case

CCNPP FC Transfer Cask			Top End Drop – 75G Load								
			Max Stress [ksi] Stress Ratio [%]			Allowable [ksi]			Material Properties [ksi]		
#	Component	Material Specification	PM	PL	PL+PB	PM	PL	PL+PB	Sy	Su	Sm
1	Structural Shell	SA-516 Type 70 Carbon Steel Plate	16.3 33.2%	17.2 27.3%	17.2 27.3%	49.0	63.0	63.0	32.6	70	21.7
2	Inner Shell	SA-240 Type 304 Stainless Steel Plate	20.3 45.1%	23.0 39.6%	23.0 39.6%	45.1	58.0	58.0	20.7	64.4	18.7
3	Top Cover Plate	SA-240 Type 304 Stainless Steel Plate	21.5 47.6%	23.8 41.1%	23.8 41.1%	45.1	58.0	58.0	20.7	64.4	18.7
4	Top Flange	SA-182 Type F304N Stainless Steel Forging	17.5 34.1%	21.3 32.3%	21.3 32.3%	51.2	65.9	65.9	22.7	73.2	20.3
5	Bottom Support Ring	SA-182 Type F304N Stainless Steel Forging	2.8 5.5%	13.6 20.7%	13.6 20.7%	51.2	65.9	65.9	22.7	73.2	20.3
6	Bottom Cover Plate	SA-240 Type 304 Stainless Steel Plate	2.6 5.7%	14.7 25.4%	14.7 25.4%	45.1	58.0	58.0	20.7	64.4	18.7
7	RAM Access Ring	SA-182 Type F304N Stainless Steel Forging	4.5 8.8%	10.5 15.9%	10.5 15.9%	51.2	65.9	65.9	22.7	73.2	20.3
8	Bottom End Plate	SA-240 Type 304 Stainless Steel Plate	3.3 7.3%	6.8 11.7%	6.8 11.7%	45.1	58.0	58.0	20.7	64.4	18.7

The standard, conservative stress screening procedure, described in Section 8.2, shows that all component stresses pass stress criteria, except of stresses at the Top Cover Plate component in the side drop event. In 75G side drop case, the original, automated stress screening procedure described in Section 8.2, has led in Top Cover Plate to stress magnitudes: 67.9 ksi - for the maximum wall averaged stress intensity, and 84.0 ksi - for the maximum surface stress intensity.

Therefore, the more thorough stress qualification for Top Cover Plate, based on the collected stress data, has been carried out that sorted out data that do not have legitimate characteristics of the ASME categories of primary stress.

Values of PM and PL stresses, and value of maximum stress intensity stress, PL+PB, obtained in the detailed stress qualification procedure pass stress criteria. These values were tabulated in Table 17, while the method used in the stress qualification is described in the following section.

In order to evade indistinctness in ASME code stress classifications due to provisional character of stress classification in case of the Top Cover Plate component, and to determine whether factual, observed stress pattern can lead to not acceptable failure mode, the collapse-load-limit-analysis was performed in accordance with rules of Appendix F of ASME code for side drop event.

The collapse-load-limit-analysis limit load value, for the side drop accident, also passed ASME code criteria (83.3G inertia load). The collapse-load-limit-analysis for the side drop accident scenario run was not showing any abnormal behavior and deterioration of solution convergence until 85G load.

8.3.2. Stress Evaluation Details

Visual presentation of stresses, in particular stresses of Top Cover Plate, is enclosed in the Appendix (Figure 12 through Figure 26). Plots show that all distinguishably higher surface stresses are localized in close proximity to the top-cover-plate-to-flange contact interfaces, as well as in the area adjacent to the side drop impact interface (15° arc with boundary conditions at lid bottom).

These stresses can be classified as the bearing stresses caused by the contact pressure load imposed on the contact interfaces, or reaction forces on impact interface. ASME code does not put a cap on bearing stresses for Service Level D conditions. Therefore, the observed stresses are deemed acceptable as the local bearing stresses as long as they do not contribute to not acceptable failure mode of Top Cover Plate, like excessive plastic deformation, or plastic hinge.

The deformation mode of Top Cover Plate is documented in Figure 13 and Figure 14. The plate deformation is showing regions of local bending near bolt heads as well as very moderate whole lid component bending. The most deformed section is the 1.5 thick bottom section of the plate in close proximity to the boundary condition region.

In order to classify obtained stresses and set up the justifiable method to sort out stresses that do not contribute to gross failure of the whole component, the Top Cover Plate stress has been analyzed separately for the following Top Cover Plate sections (Figure 30):

- 1.5 inch thick outer sections, numbered 1 through 9, representing vent opening segments,
- 2.5 inch thick outer sections, A through H, representing bolt fastening segments,
- 3.0 inch thick Central Section; main part of lid for which deformation and stresses are of primary concern to overall failure.

Figure 31 through Figure 33 show the wall averaged stresses and the surface stresses, collected from all qualification paths (Figure 29).

One can note that all distinguishably high stresses for Sections 1-9 are bearing stresses, occurring at the impact-boundary-conditions area (Section 9), or the stresses induced by structural discontinuity at the close proximity to the onset of boundary conditions area (Section 8). These stresses and deformations are deemed very local and are transferred directly to the central part of the lid, while bearing stress magnitudes are not limited for Service Level D conditions.

The stresses for sections A through H are also moderate, except for the bearing load areas (Sections A, B and H). The highest stress level is observed in section H. These high magnitude stresses are localized around the region of bottom bolt hole and are caused by bolt hole deformation due to its proximity of impact interface.

The deformation and stresses can be deemed local and do not contribute directly to gross deformation of the lid. The presence of a bolt hole close to the impact interface is softening the lid structure at its bottom. Therefore the deformation and stresses at lid concentrate at its bottom section H in the vicinity of the bolt hole.

Detailed examination of collected stress data indicate that the effect of the bolt hole deformation starts at circumferential area θ = 163.2 and ends at θ = 173.7. Therefore, stresses generated in Central Section at this angle sector, at its vicinity to Outer Section H (radial coordinate 33.2 through 34.9), should not be considered in the classification of primary general membrane stress intensity PM, although they need to be reviewed as the potential local primary stresses, PL.

Therefore using wall averaged stress data, illustrated on Figure 31 through Figure 33, one can obtain realistic estimation for primary general membrane stress PM=35288.9 psi, and using surface stress data one can obtain maximum stress intensity, PM/PL+PB = 47904.6 psi.

The postulated envelope for primary local membrane stress is PL=45429.0 psi. That magnitude is based on the wall averaged stress for lid Central Section obtained at the interface of Central Section with Outer Section H, that is deemed characteristic and dominated stress level at that interface.

The table below documents path information data for stress values PM, PL, and PL+PB described above:

Stress Category	Stress Value [psi]	Circumferential Coordinate θ (*) [deg]	Vertical Coordinate X [in]	Radial Coordinate R (*) [in]
PM	35,288.9	162.0	9.6	32.0
PL	45,429.0	167.3	7.3	33.5
PM+PB	47,904.6	180.0	9.2	30.8

Note (*): ANSYS coordinate system.

Due to provisional character of the determination process of ASME code primary stress values, and to expose definitively whether primary stress pattern can lead to not acceptable failure mode, the collapse limit load analysis was performed in accordance with rules of Appendix F of ASME code for the side drop event.

The collapse-load-limit-analysis for the side drop accident scenario run was not showing any abnormal behavior and deterioration of solution convergence until 85G load. At 85.48G, last saved converged solution has been obtained. Such magnitude of collapse load secures sufficient safety margin with regard to postulated nominal 75G load. As it is estimated in Section 5, collapse load for cask design needs to exceed 83.3G inertia load to pass ASME code criteria.

Obtained estimation of 85G for collapse load is deemed conservative, because the observed cause of convergence failure of collapse-load-limit-analysis at loads exceeding 85G appeared the local deformation of bolt hole at close proximity to impact interface, exceeding application range of RBE3 type of constraints equations.

The stress and displacement status during collapse load analysis is documented in Figure 20 and Figure 19, respectively. The plots confirm that even the high local stresses do not cause Top Cover Plate collapse.

The effect of the prying action of Top Cover Plate (due to its deformation) onto the plate bolts in the result of 75G side drop can be estimated by analyzing magnitudes of axial forces in the bolts. The table below presents bolt forces (output quantity SMISC1 for COMBIN39 elements) of all bolts of the Top Cover Plate. Pictorial presentation of the tabulated forces and bolt elements is provided in the Figure 34. The table shows also bolt average tensile stresses (per Table 10, bolt tensile cross section A_{ten} = 1.8712 in^2 was used in the stress determination) and compares these stresses to bolt stress allowable.

Bolt Number	Bolt Circumferential Coordinate	Bolt Element Number	Bolt Tensile Force	Average Tensile Stress	Stress Ratio (1) [%]
1	11.25	125664	87113	46554	53.2%
2	33.75	125668	74701	39921	45.6%
3	56.25	125672	49011	26192	29.9%
4	78.75	125676	24894	13303	15.2%
5	101.25	125680	14356	7672	8.8%
6	123.75	125684	8191.9	4378	5.0%
7	146.25	125688	43010	22985	26.3%
8	168.75	125692	163170	87199	99.7%

Note 1: Ratio of average tensile stress to average tensile stress allowable min(Sy,0.7Su)=87.5 ksi [3].

One can notice that the particularly high force is exerted onto the bottom bolt (bolt number 8), generating bolt stress magnitude close to the stress allowable (stress ratio 99.7%). It is presumed that this bolt can fail. Tensile forces of all other bolts are significantly lower. One can anticipate, therefore, that growing local deformation of Top Cover Plate can cause no more than two bottom bolts to fail under prying loads and in result that Top Cover Plate can locally separate from the flange at the impact region. Such consequences of the 75G impact are deemed acceptable.

Due to the oversized 1.88 inch bolt holes, the Top Cover Plate does not depend on bolts to resist transverse shear loads. Therefore bolts are not loaded in shear and, as the result, shear loads and bending are not the design consideration.

9. Conclusions

The calculation has been construed to validate the design of NUH32PHB cask for the accident condition 75G side drop and 75G end drop scenarios. The detailed results and stress qualification discussion is documented in Section 8.3. The calculation shows that new design version of Top Cover Plate, allowing for vent openings, satisfies ASME code criteria for the analyzed events.

10. Appendix

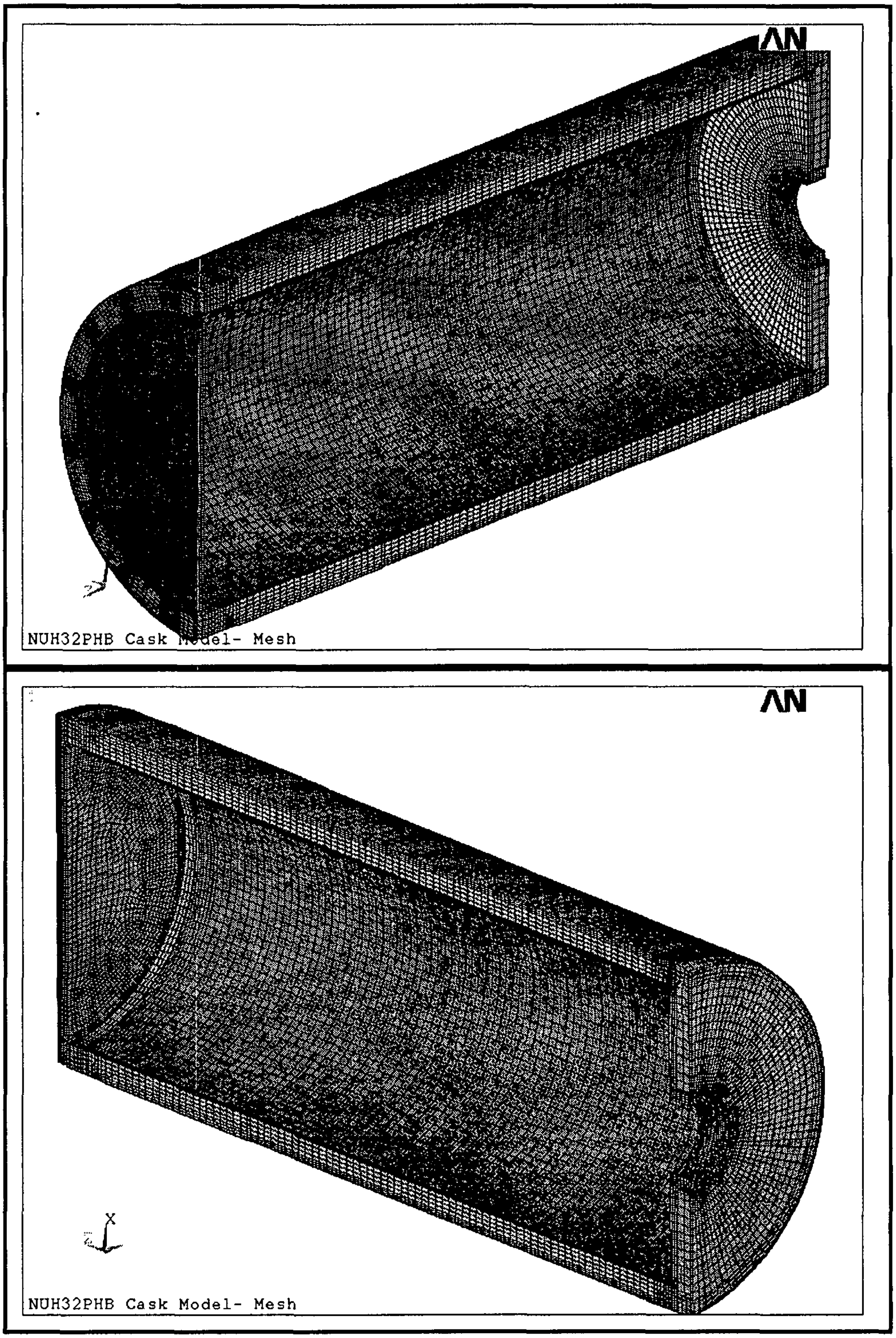

Figure 3 NUHOMS 32PHB Model – Mesh – General View

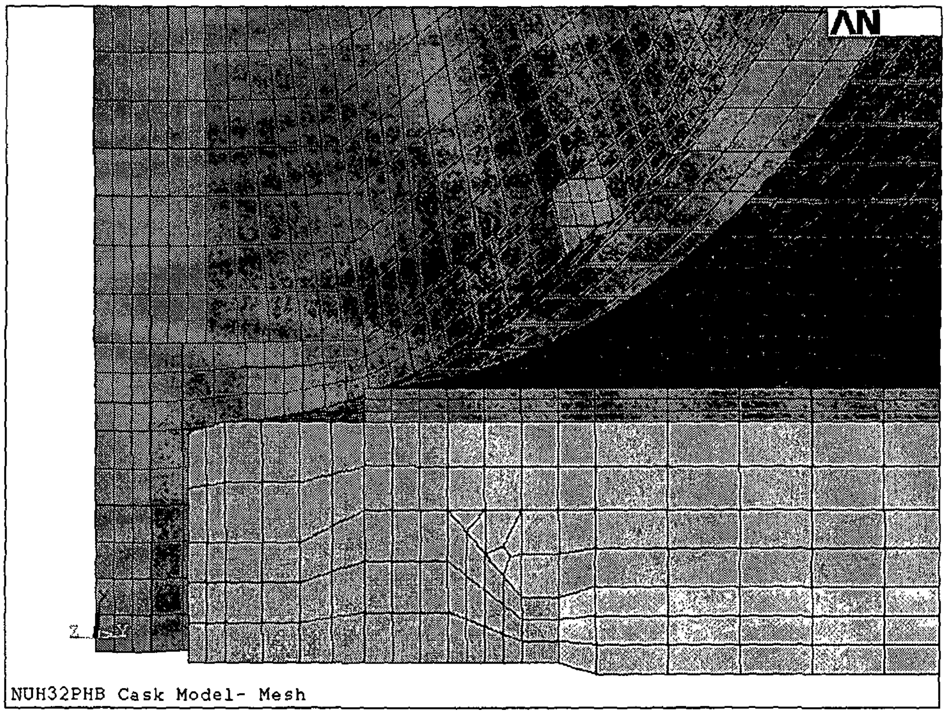

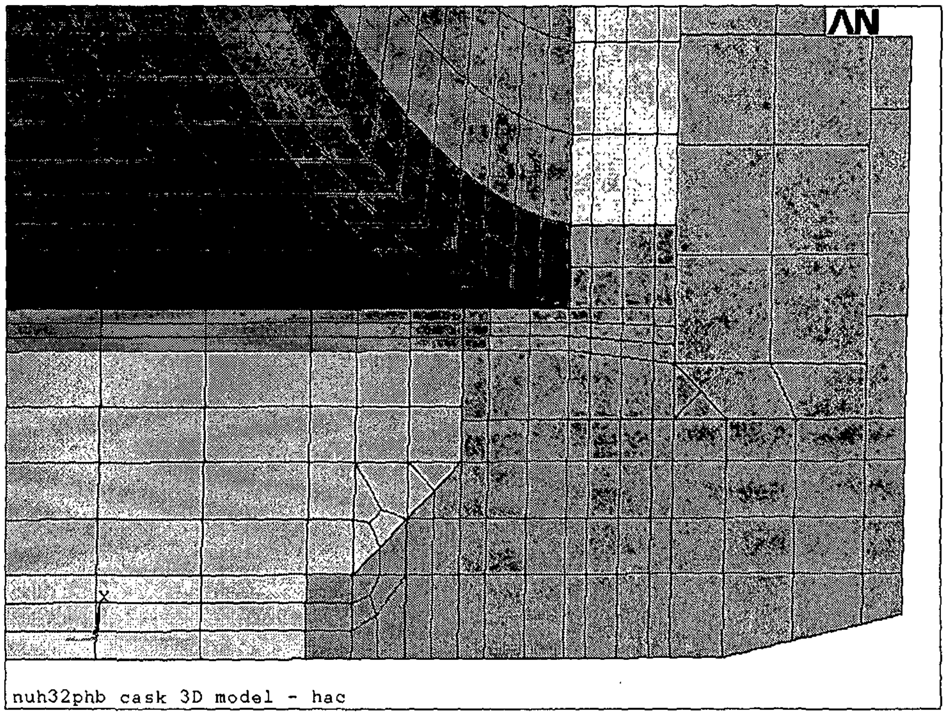

Figure 4 NUHOMS 32PHB Model – Mesh Details – Top & Bottom of Cask

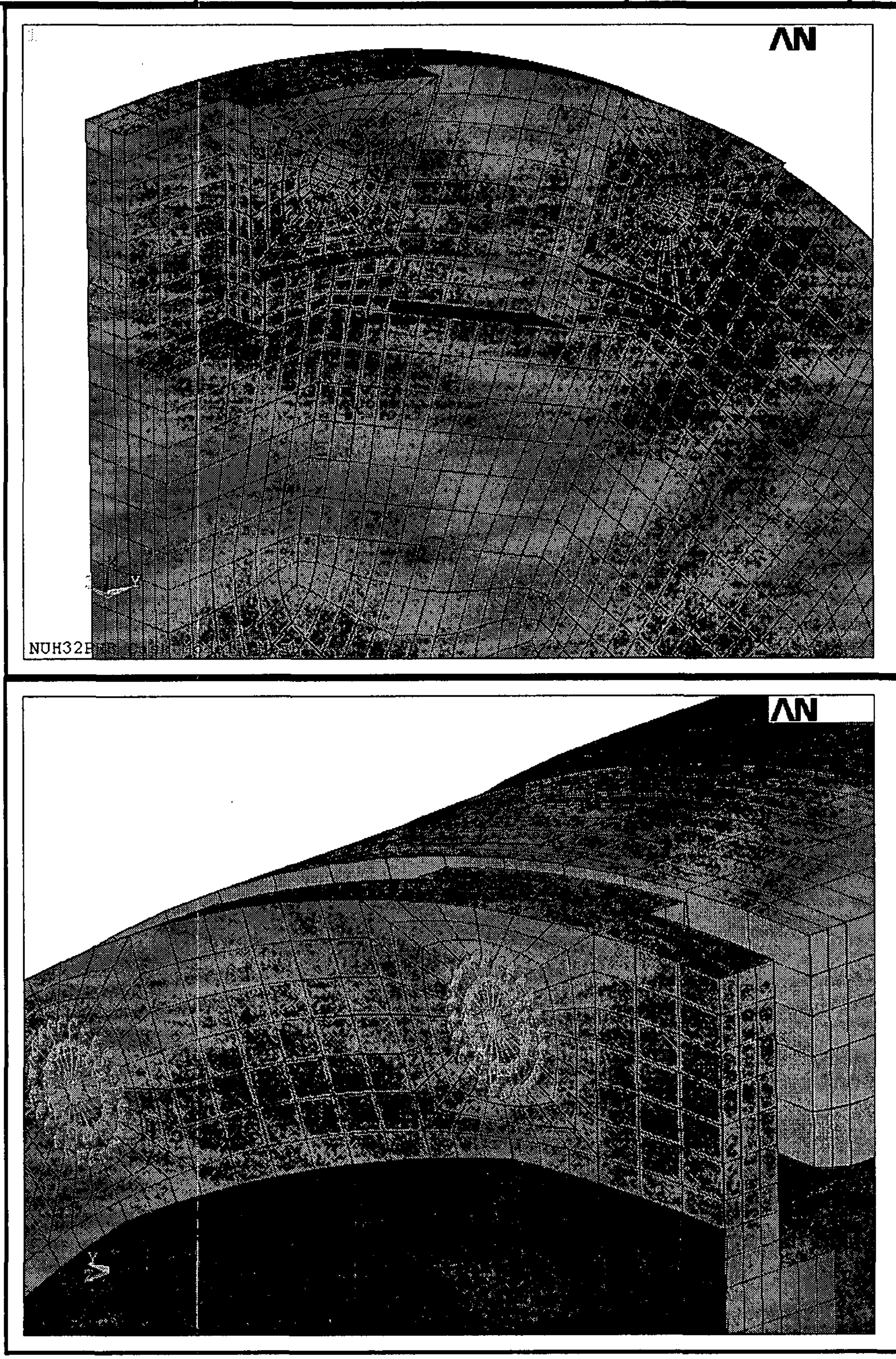

Figure 5 NUHOMS 32PHB Model – Mesh Details – Top Cover Plate Area

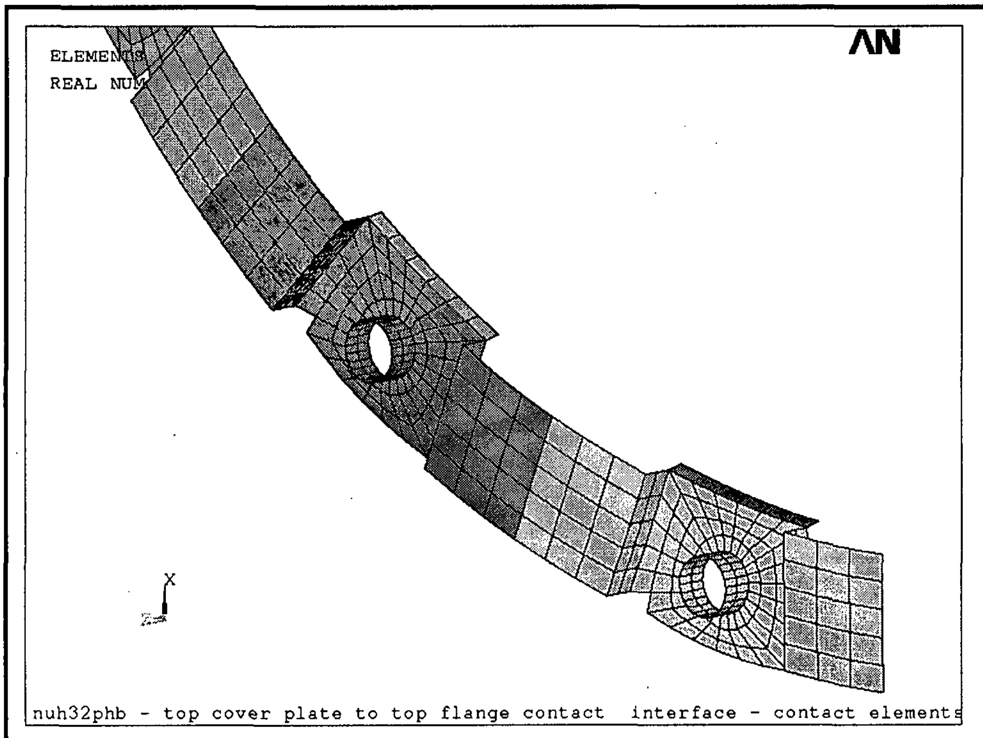

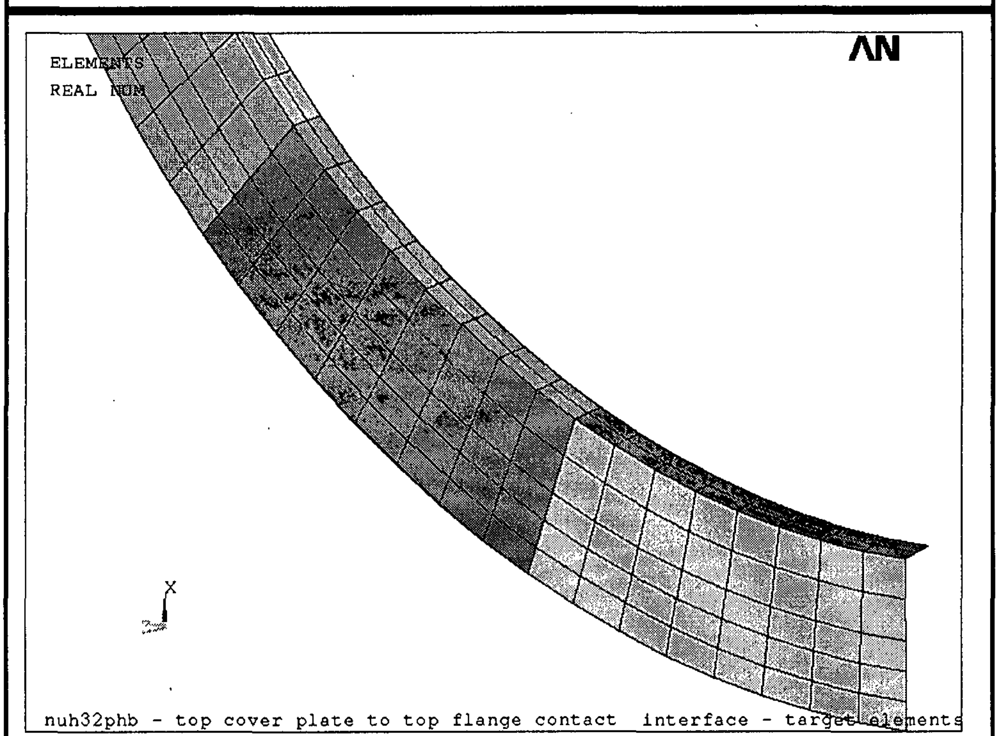

Figure 6 Top Cover Plate Interface – Contact Elements & Target Elements

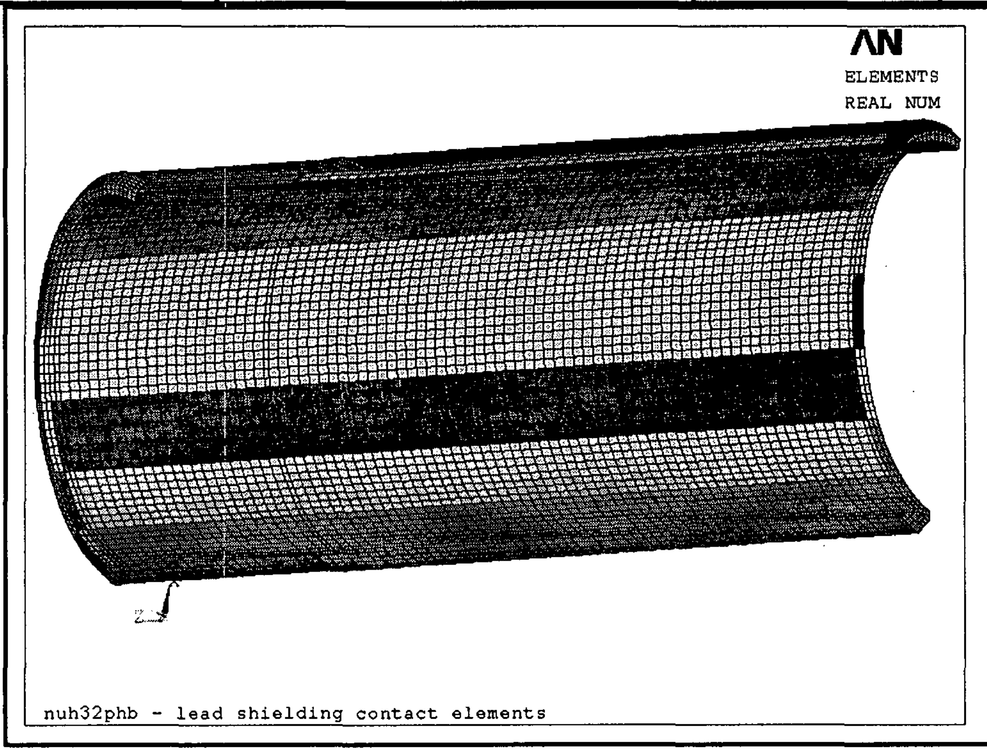

Figure 7 Lead Shielding Contact Elements

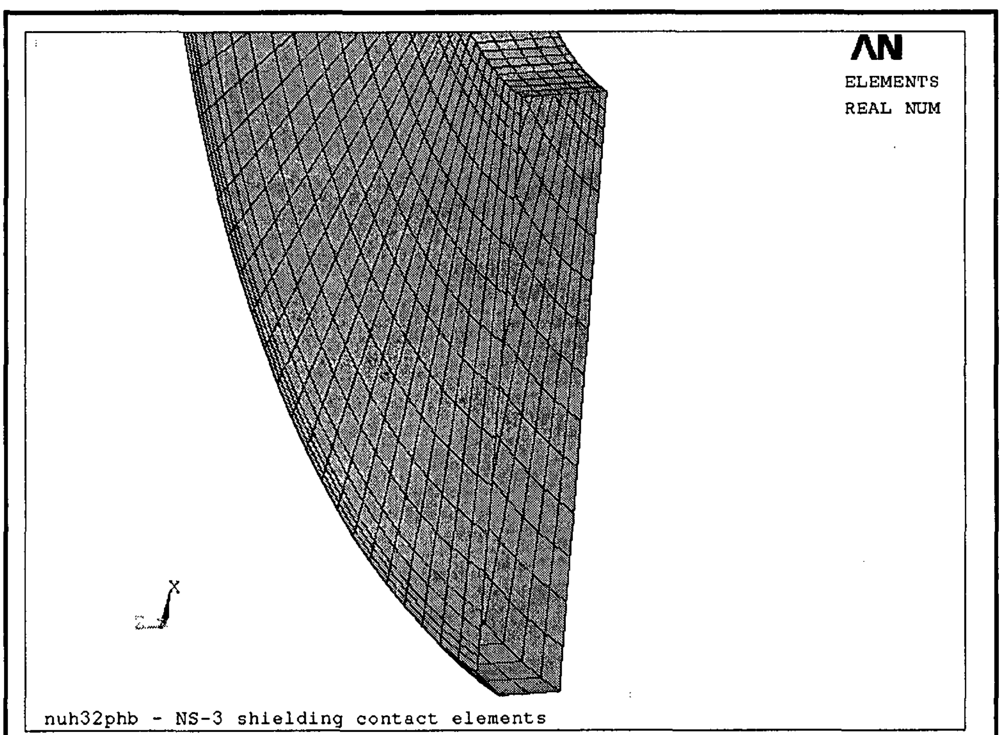

Figure 8 NS-3 Shielding Contact Elements

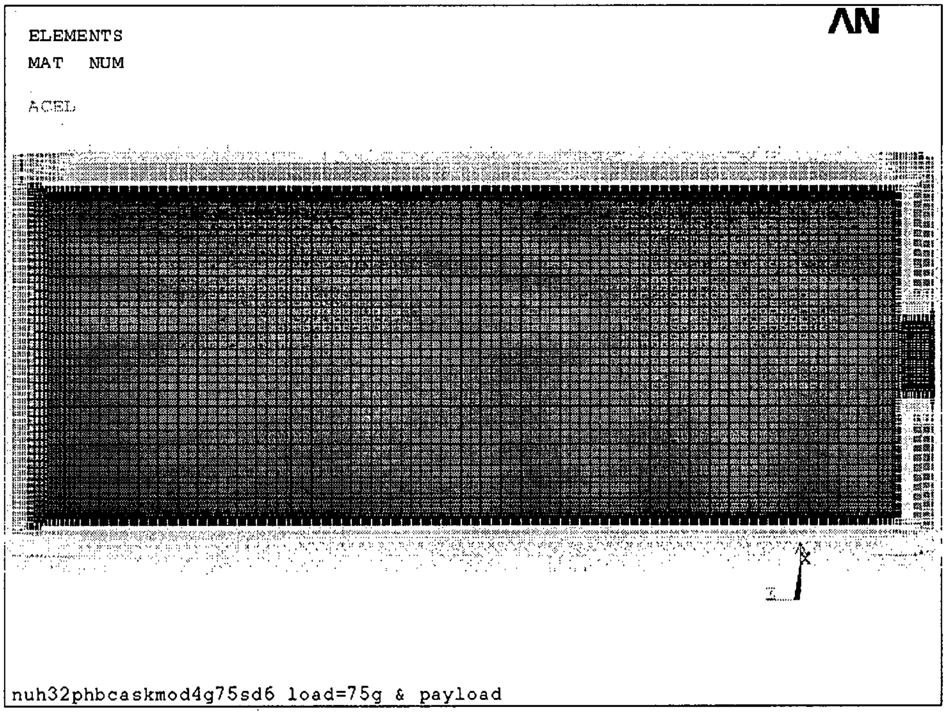

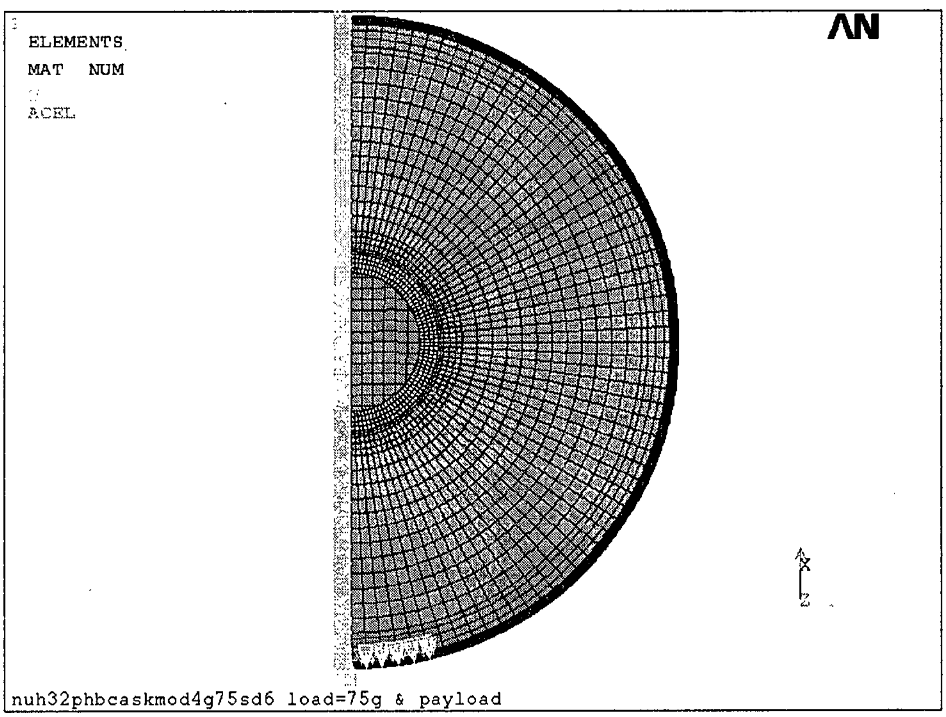

Figure 9 Side Drop Boundary Conditions

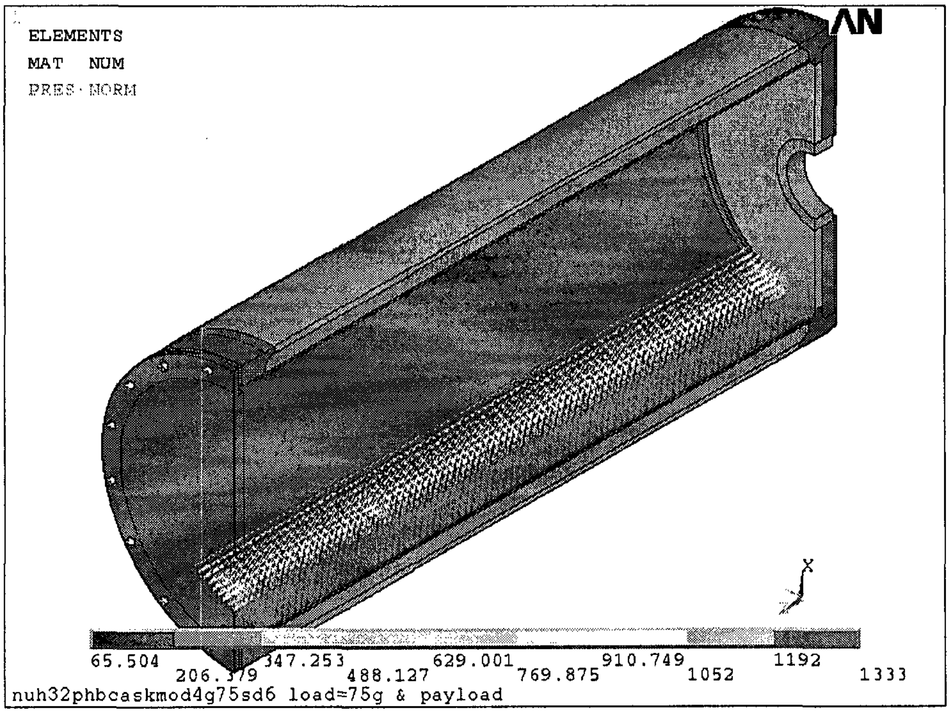

Figure 10 Side Drop Pressure Load Distribution

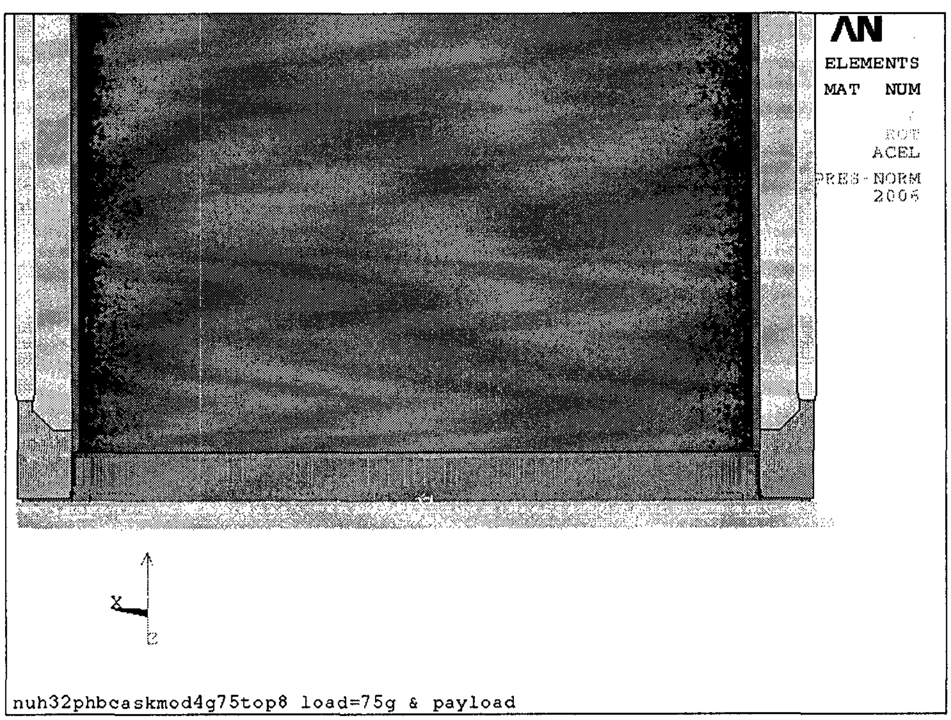

Figure 11 Top End Drop Pressure Load Distribution & BC

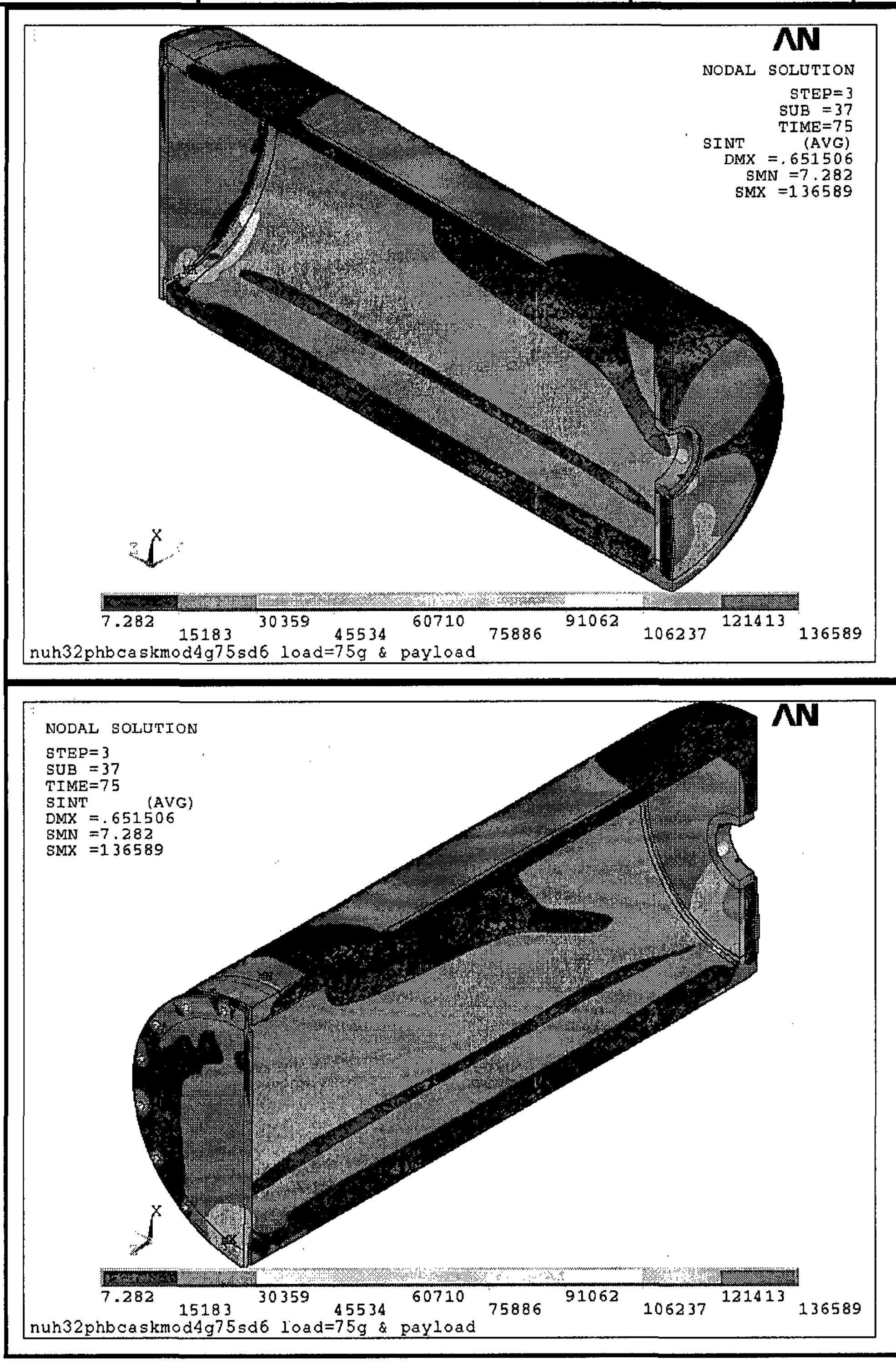

Figure 12 75G Side Drop Results – Overall Stress Distribution

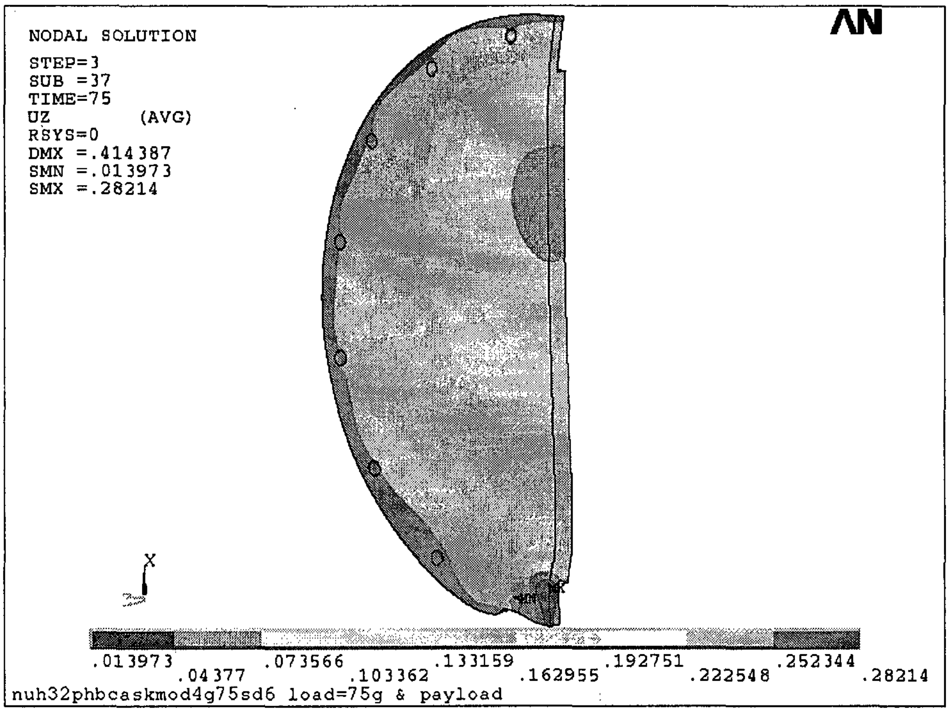

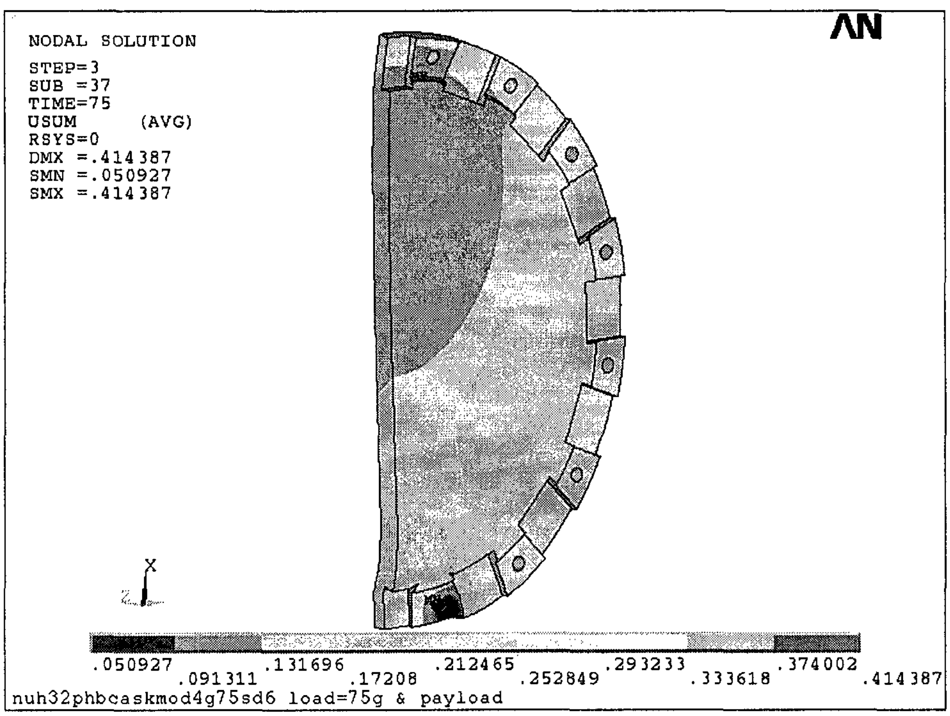

Figure 13 75G Side Drop Results - Deformation Mode

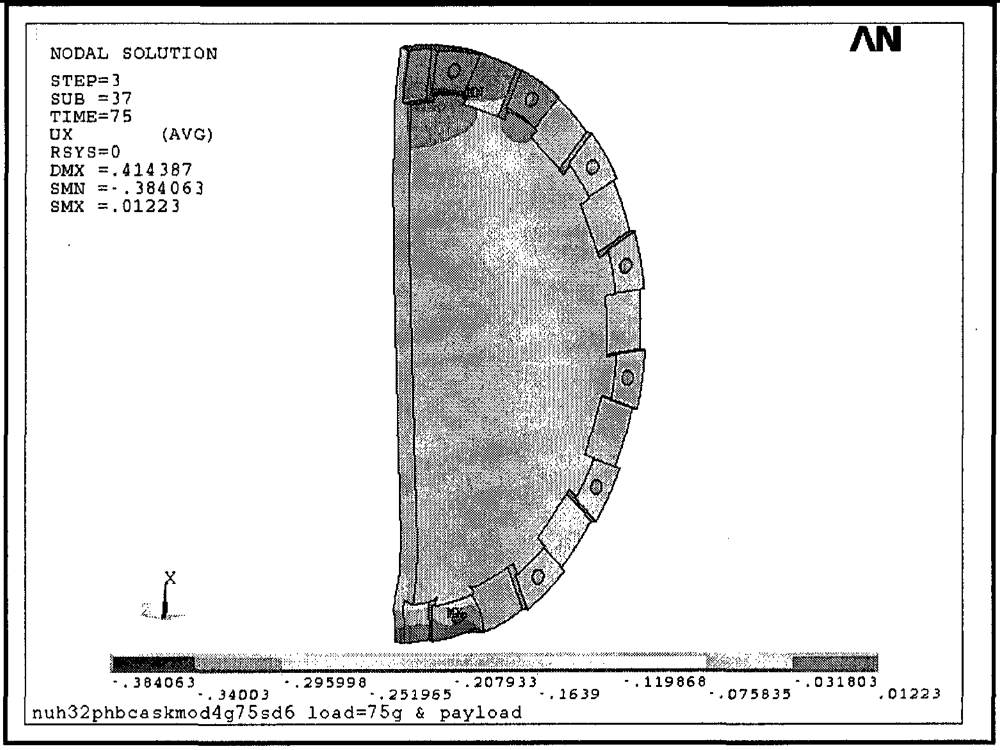

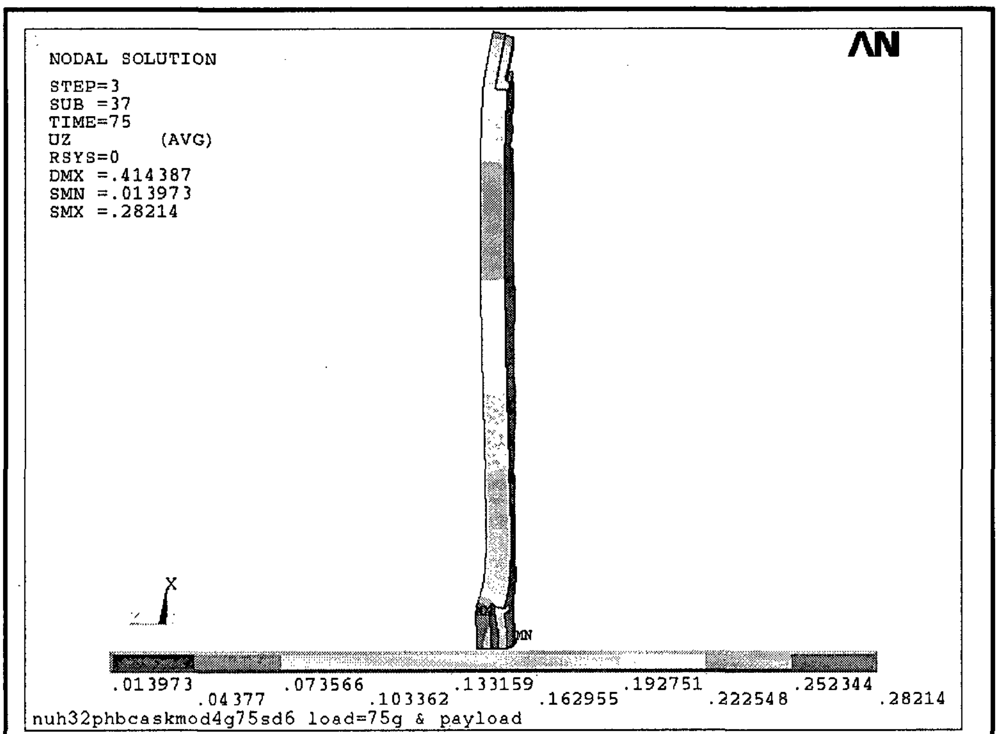

Figure 14 75G Side Drop Results - Deformation Mode (cd)

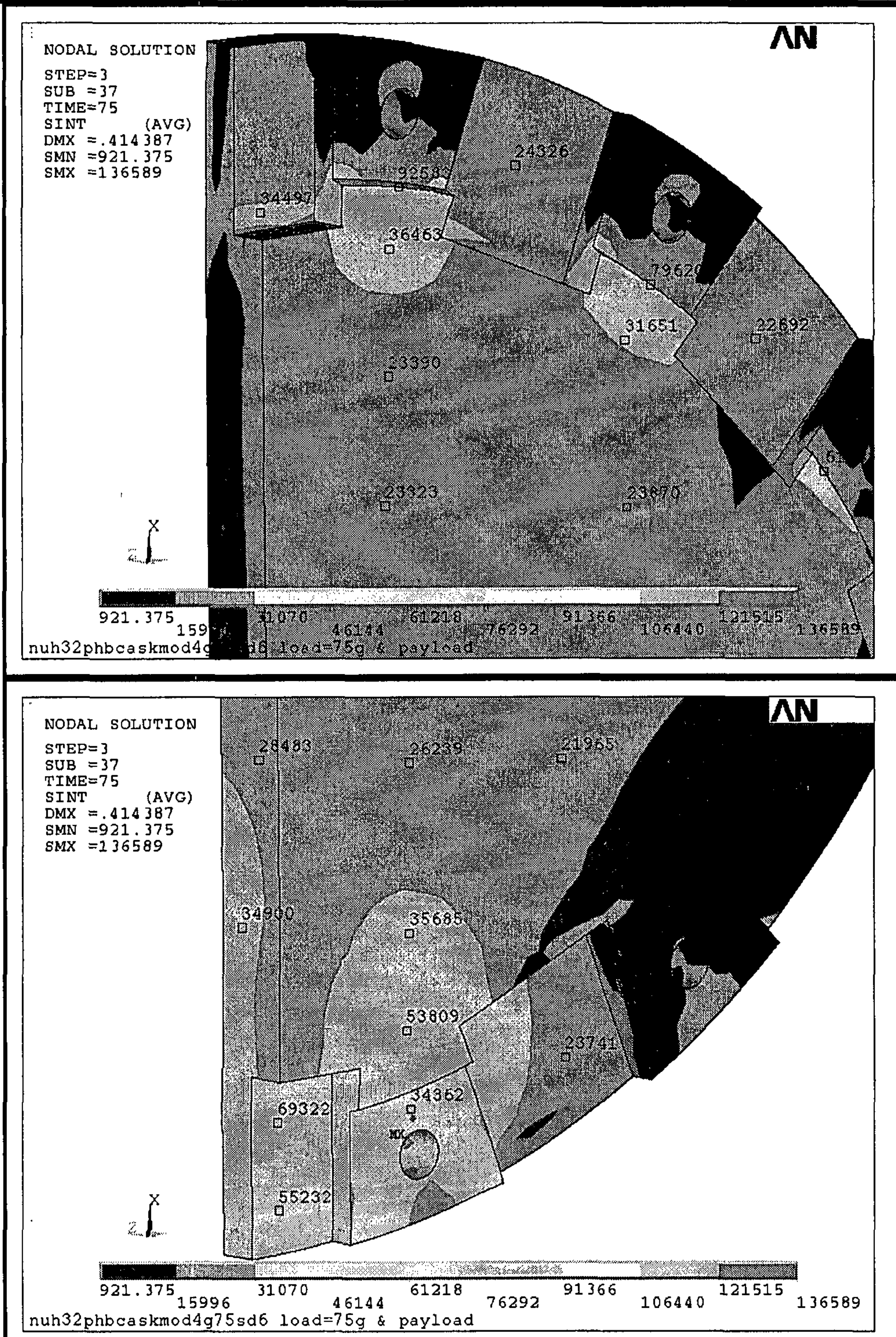

Figure 15 75G Side Drop Results – Top Cover Plate Inner Side - Surface Stress

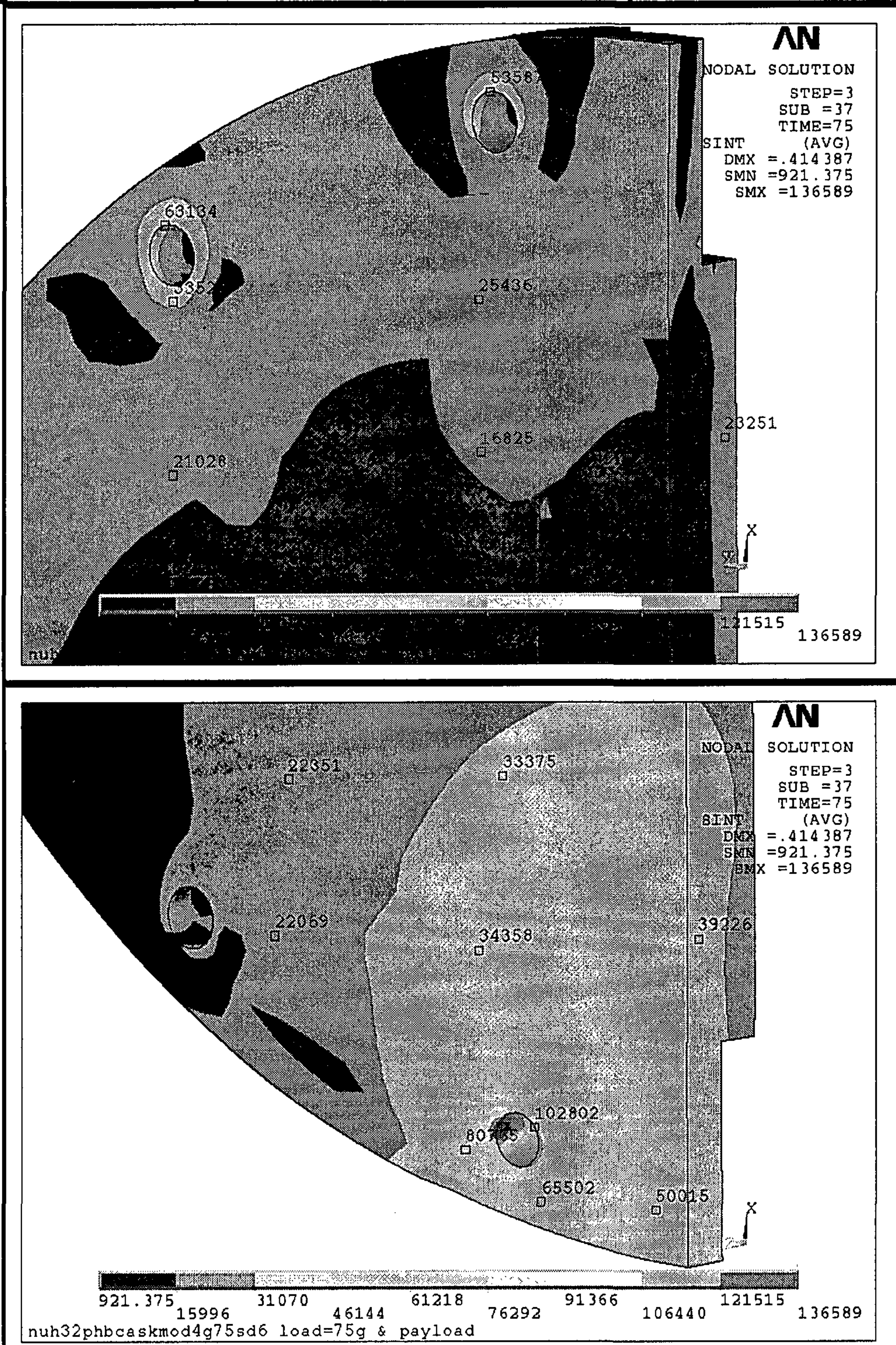

Figure 16 75G Side Drop Results – Top Cover Plate Bottom Side - Surface Stress

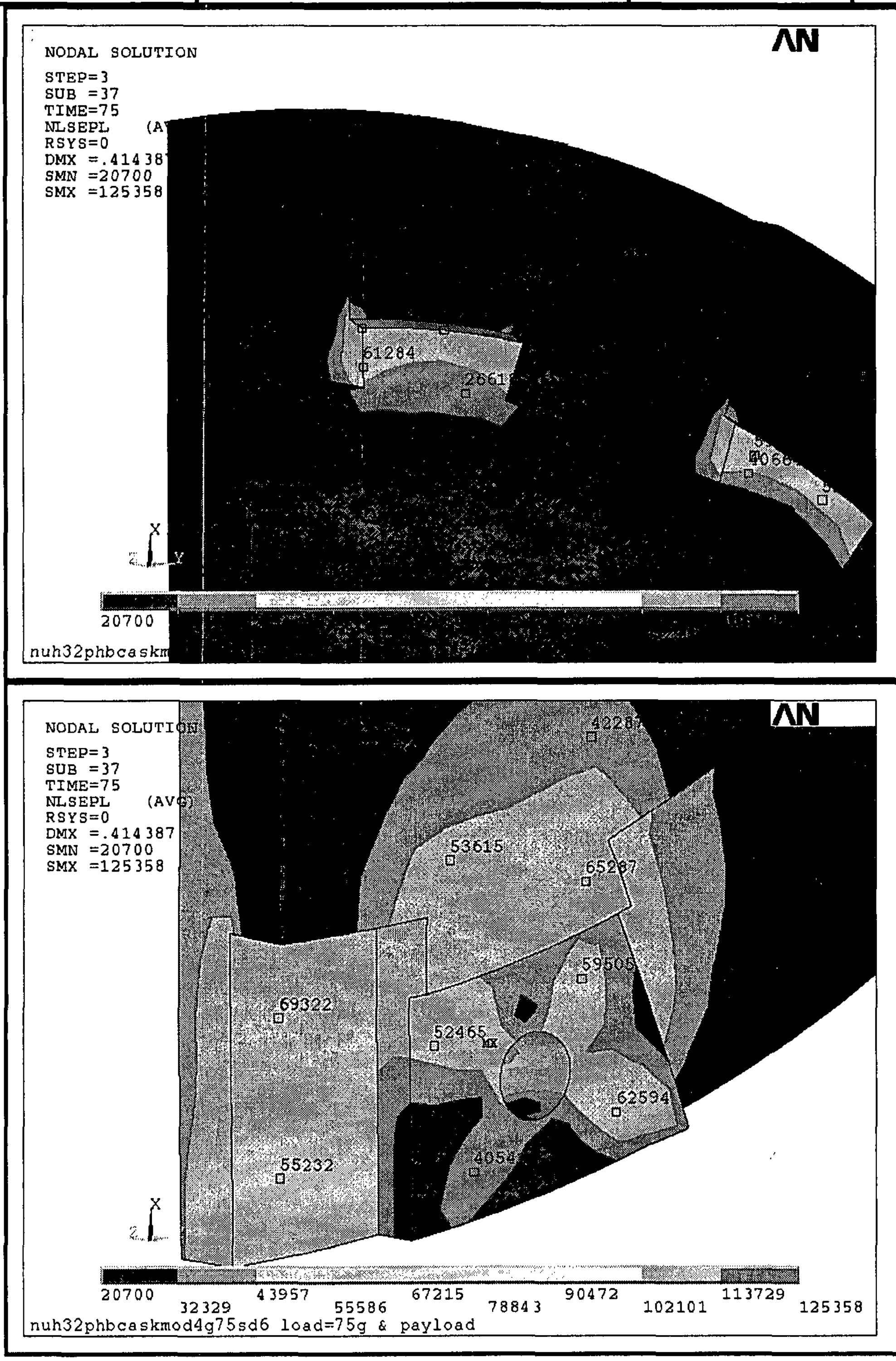

Figure 17 75G Side Drop Results – Top Cover Plate – Plastic Stress NLSEPL

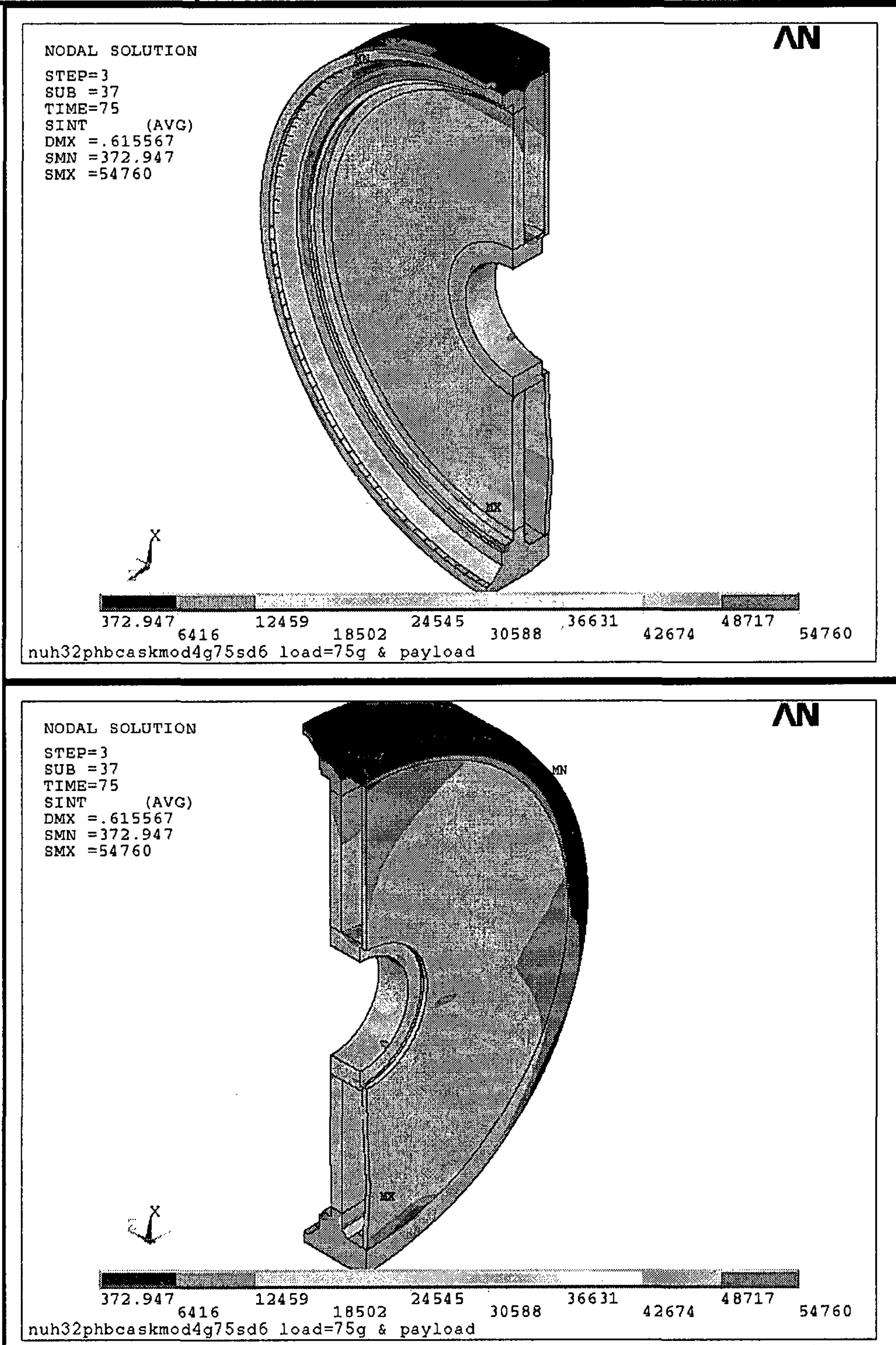

Figure 18 75G Side Drop Results – Cask Bottom Assembly - Surface Stress

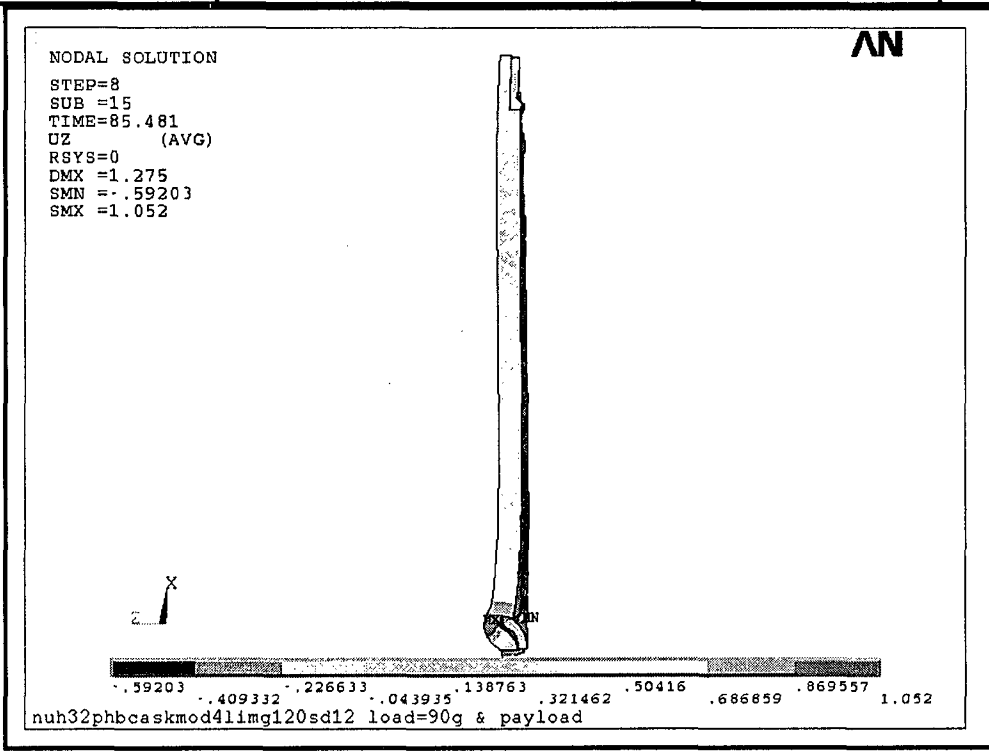

Figure 19 85.48G Side Drop Limit Analysis Results - Top Cover Plate - Deformation Mode

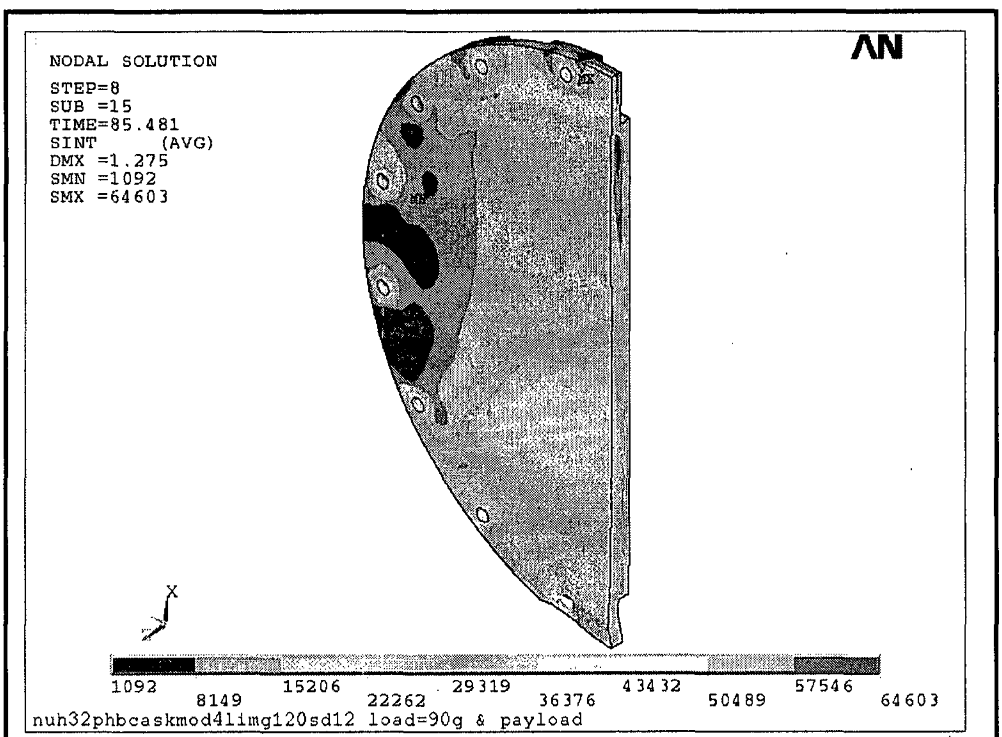

Figure 20 85.48G Side Drop Limit Analysis Results - Top Cover Plate - Surface Stress

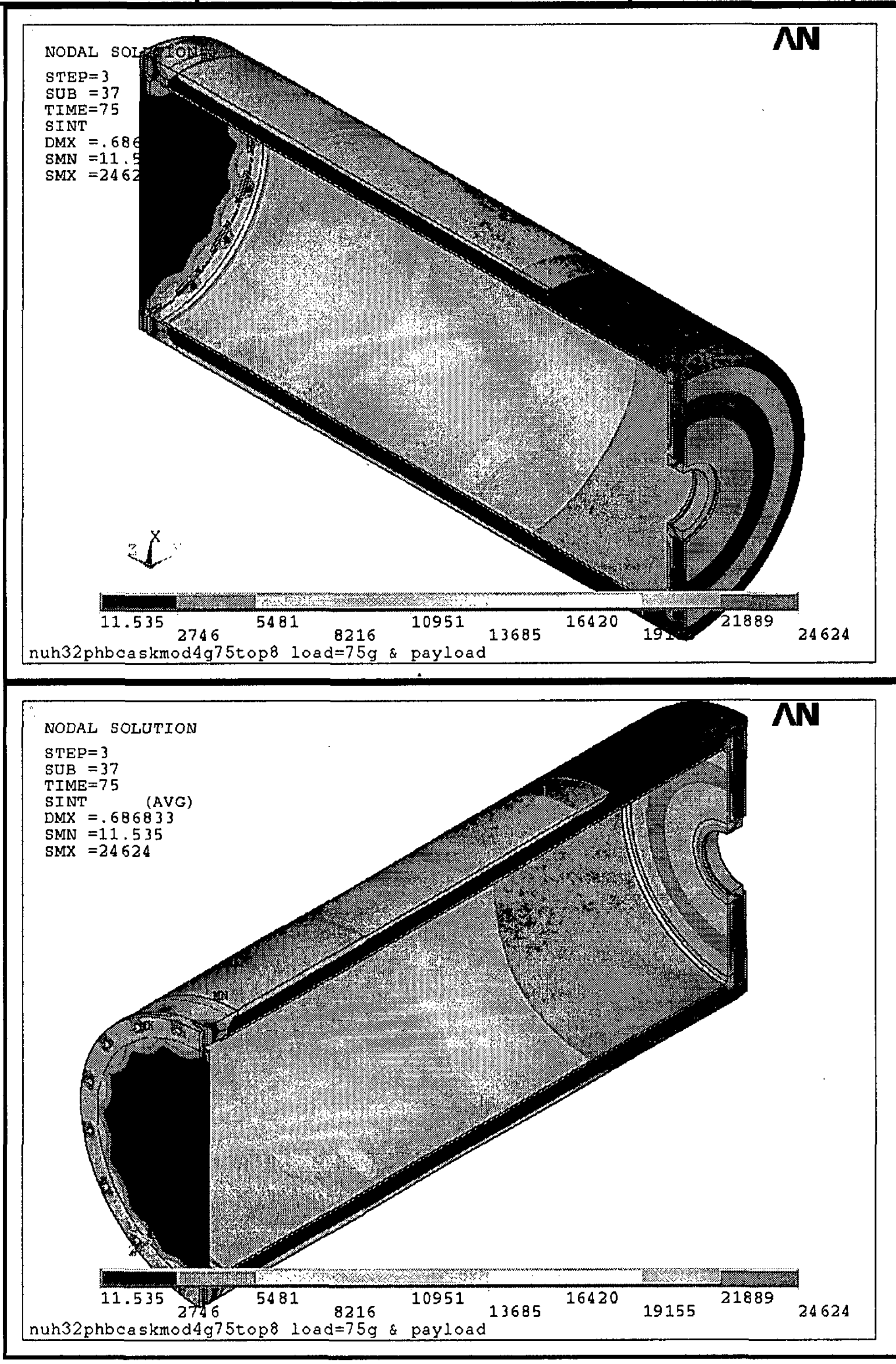

Figure 21 75G Top End Drop - Surface Stress Distribution – Overall View

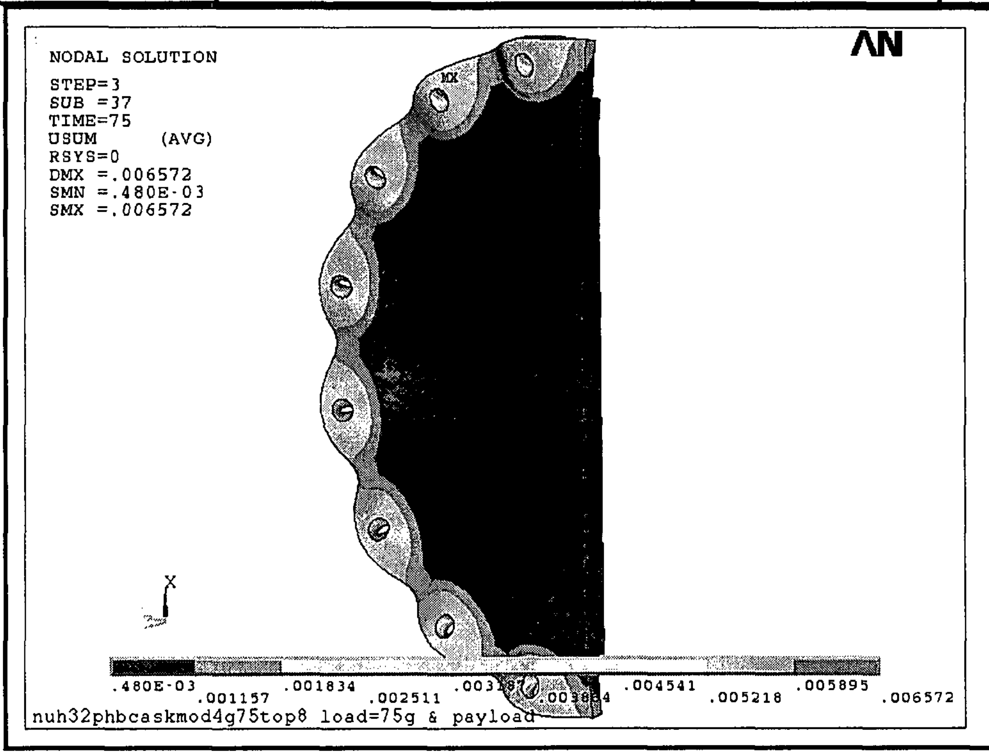

Figure 22 75G Top End Drop – Top Cover Plate - Deformation Mode

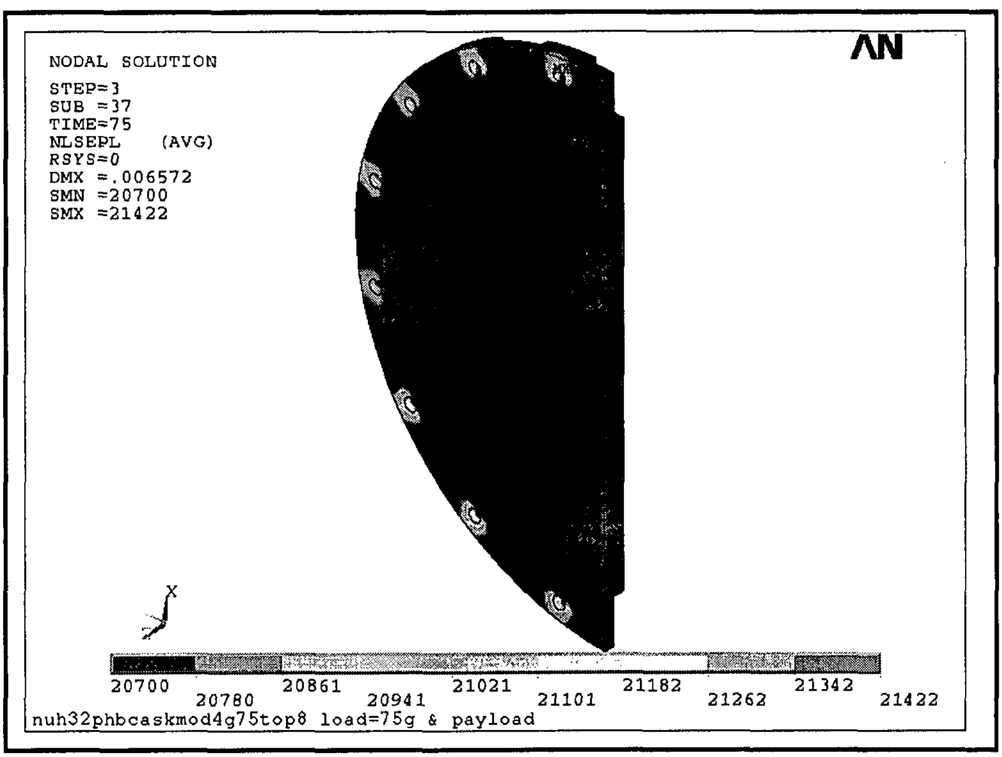

Figure 23 75G Top End Drop – Top Cover Plate – Plastic Stress NLSEPL

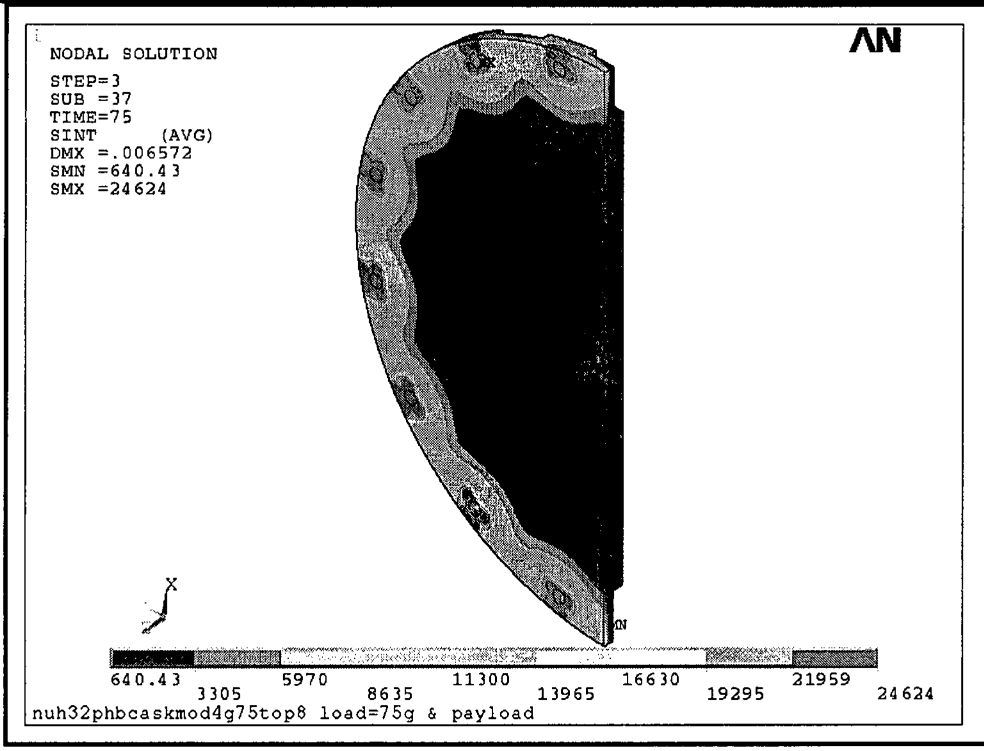

Figure 24 75G Top End Drop – Top Cover Plate – Surface Stress

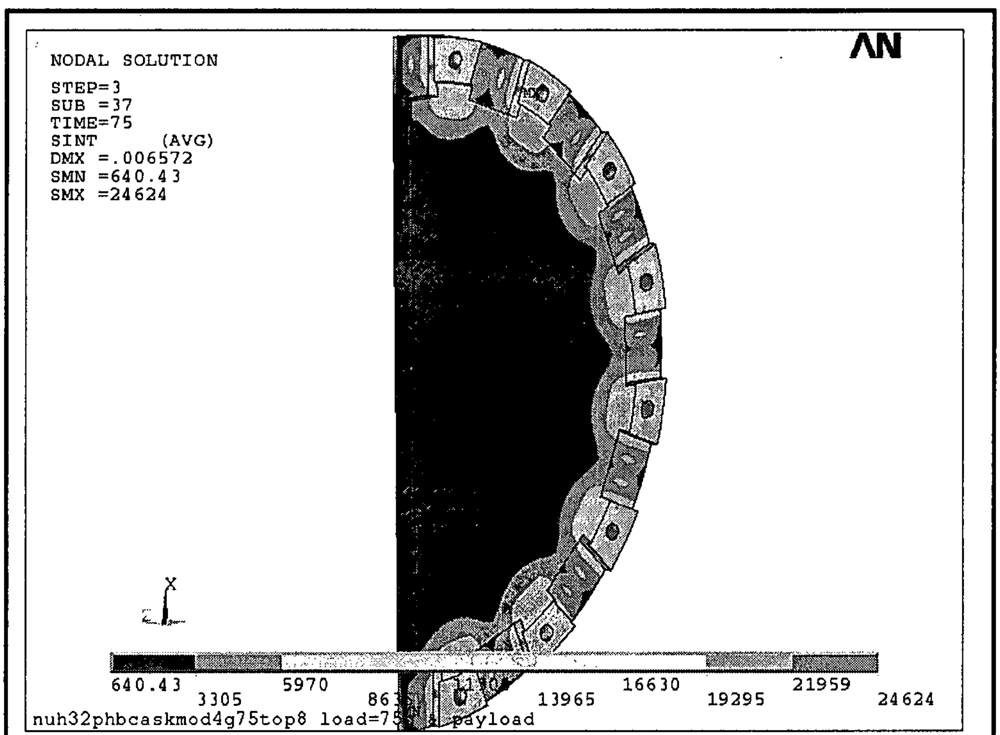

Figure 25 75G Top End Drop – Top Cover Plate – Surface Stress

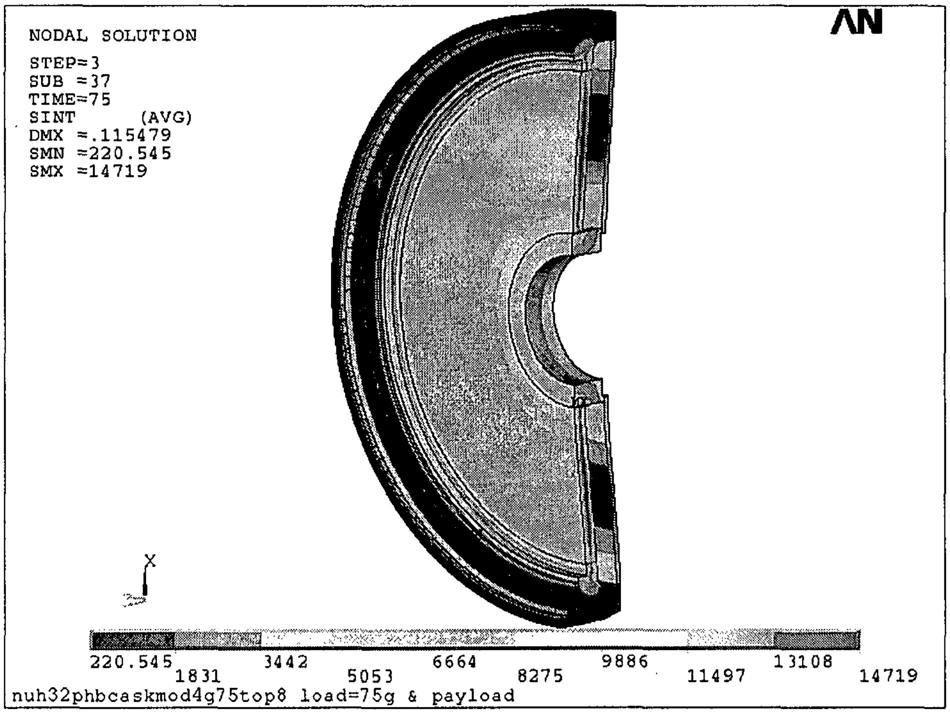

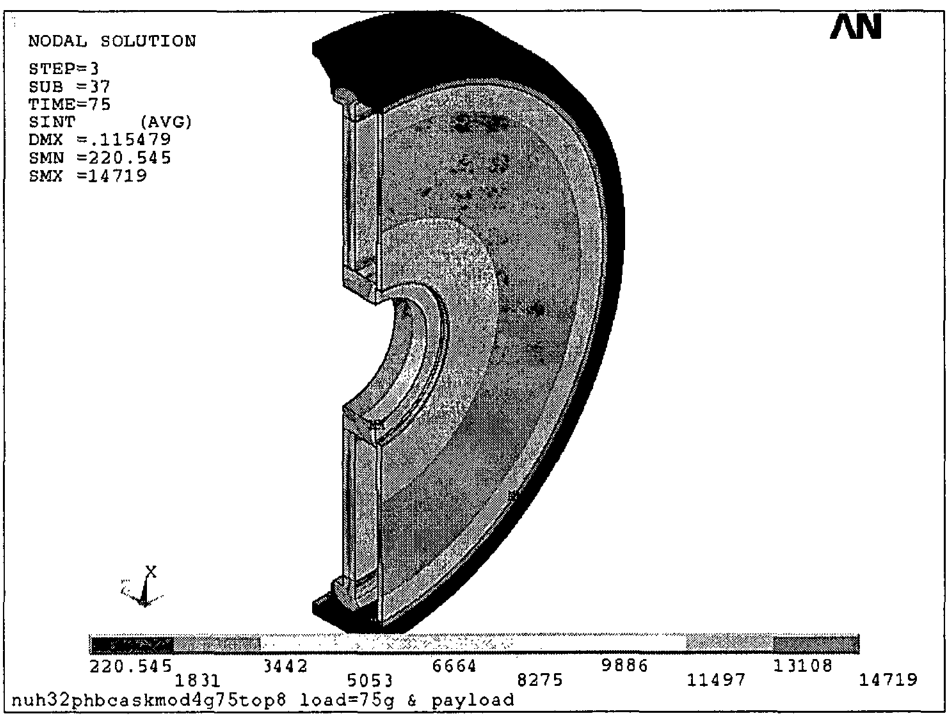

Figure 26 75G Top End Drop – Cask Bottom Assembly – Surface Stress

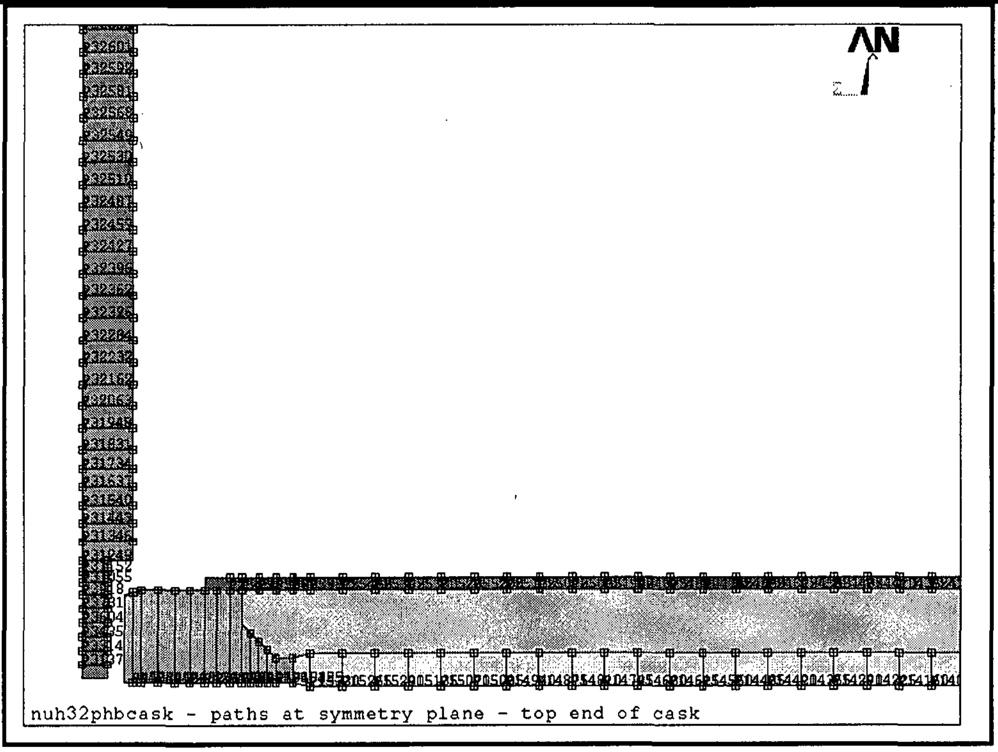

Figure 27 Stress Classification Paths – Symmetry Plane – Top End of Cask

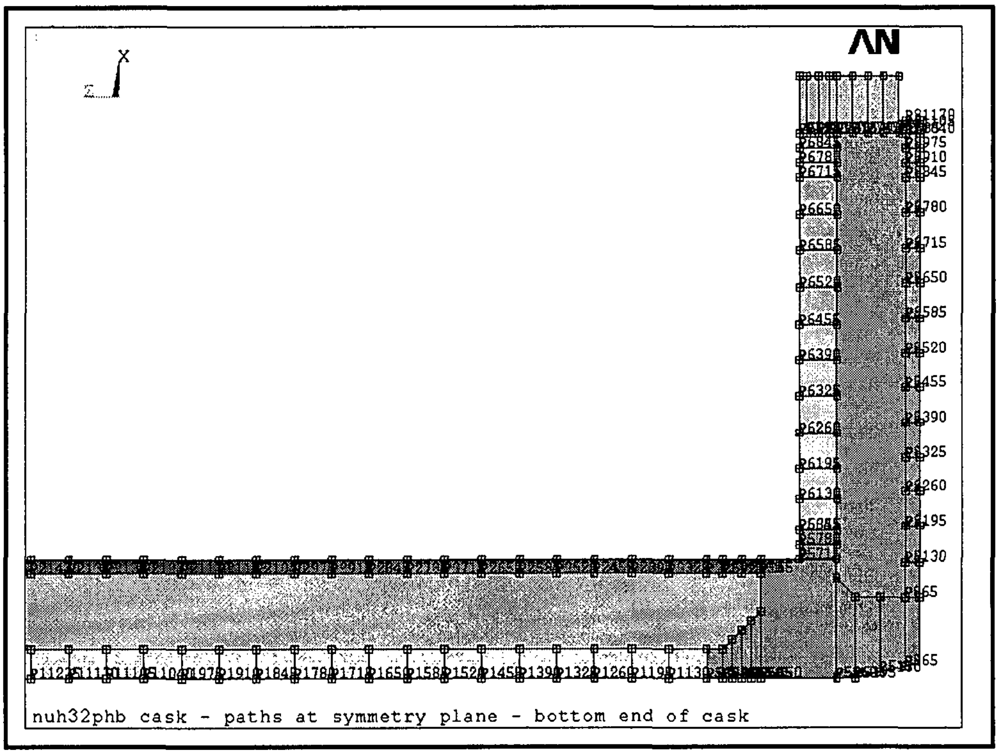

Figure 28 Stress Classification Paths – Symmetry Plane – Bottom End of Cask

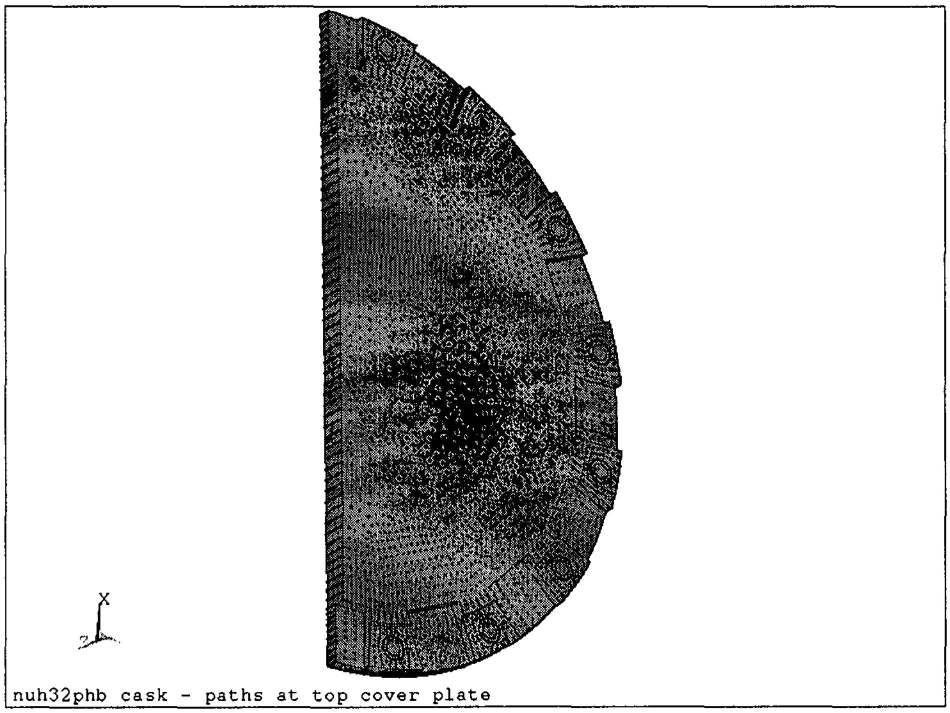

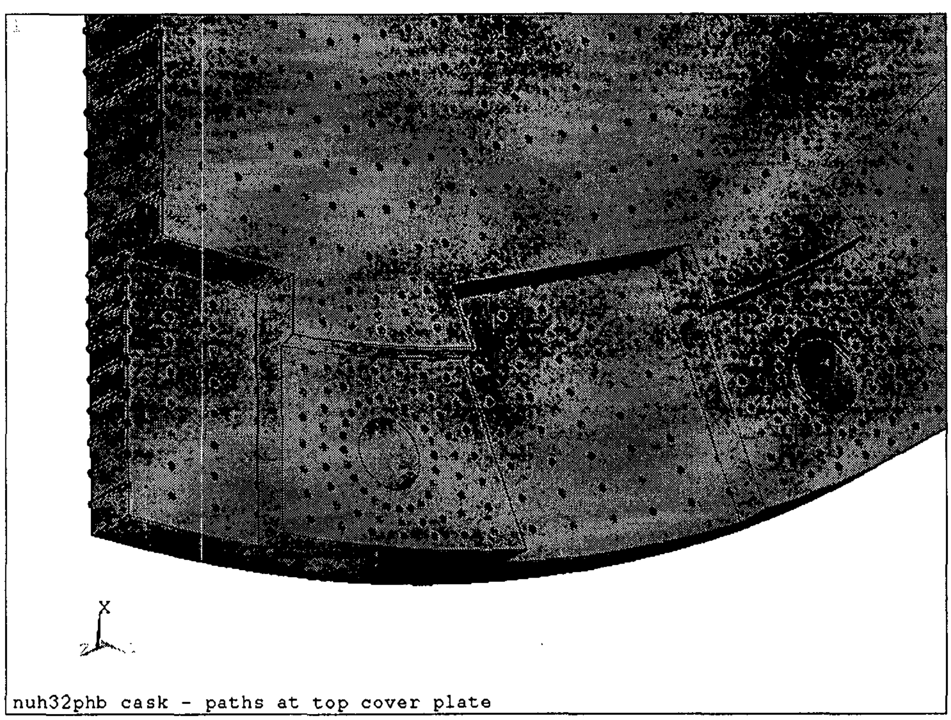

Figure 29 Stress Classification Paths – Top Cover Plate

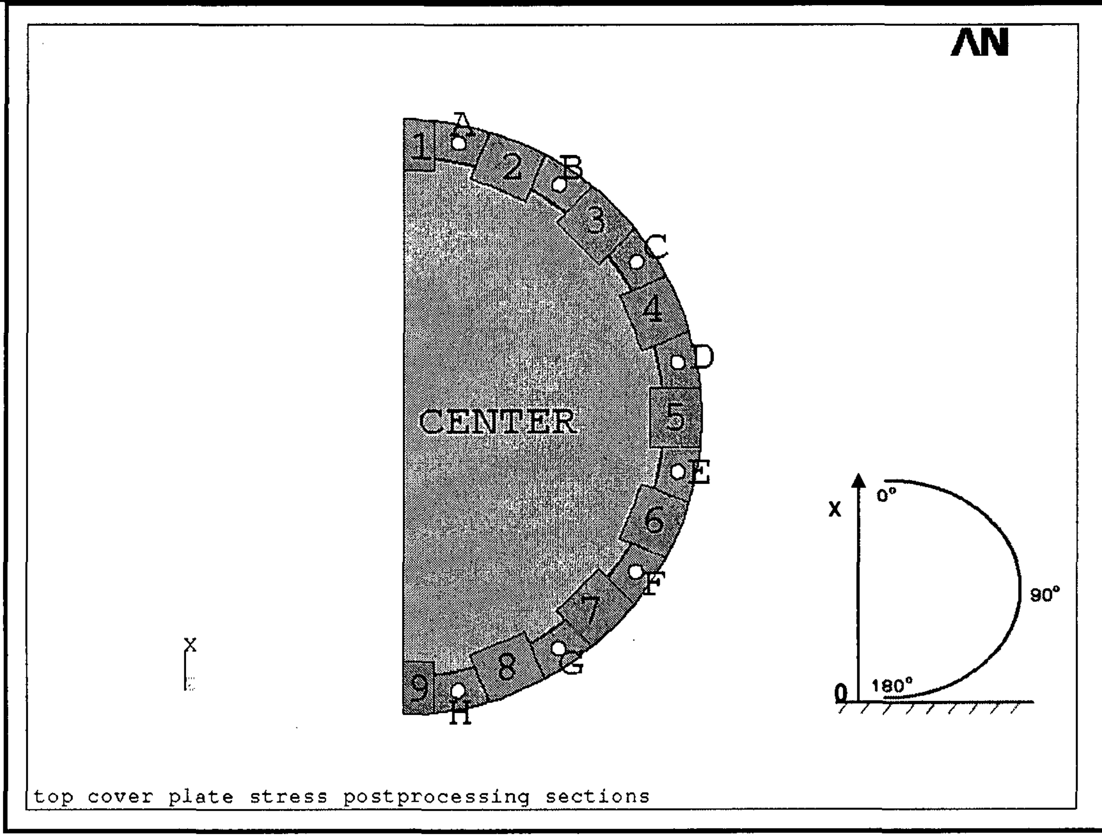

Figure 30 Stress Classification Paths Sections at Top Cover Plate

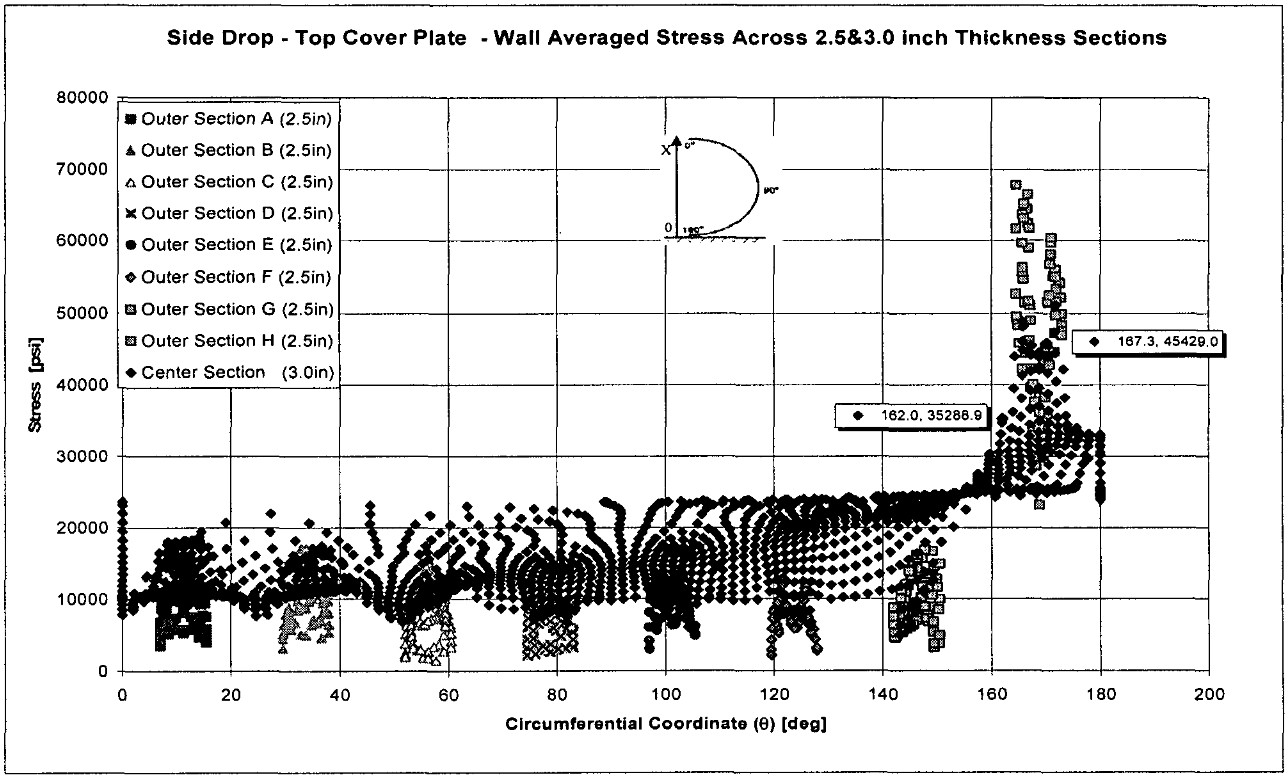

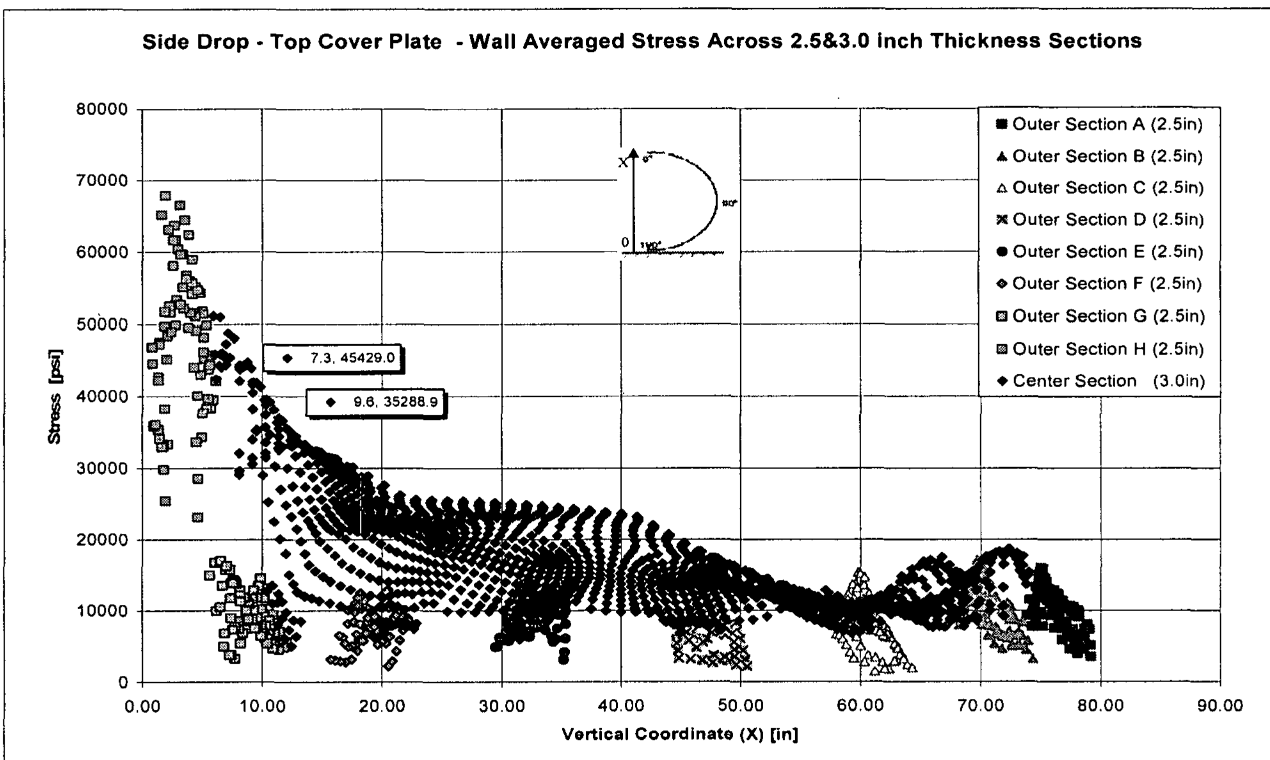

Figure 31 Top Cover Plate - Wall Averaged Stress at Predefined Sections

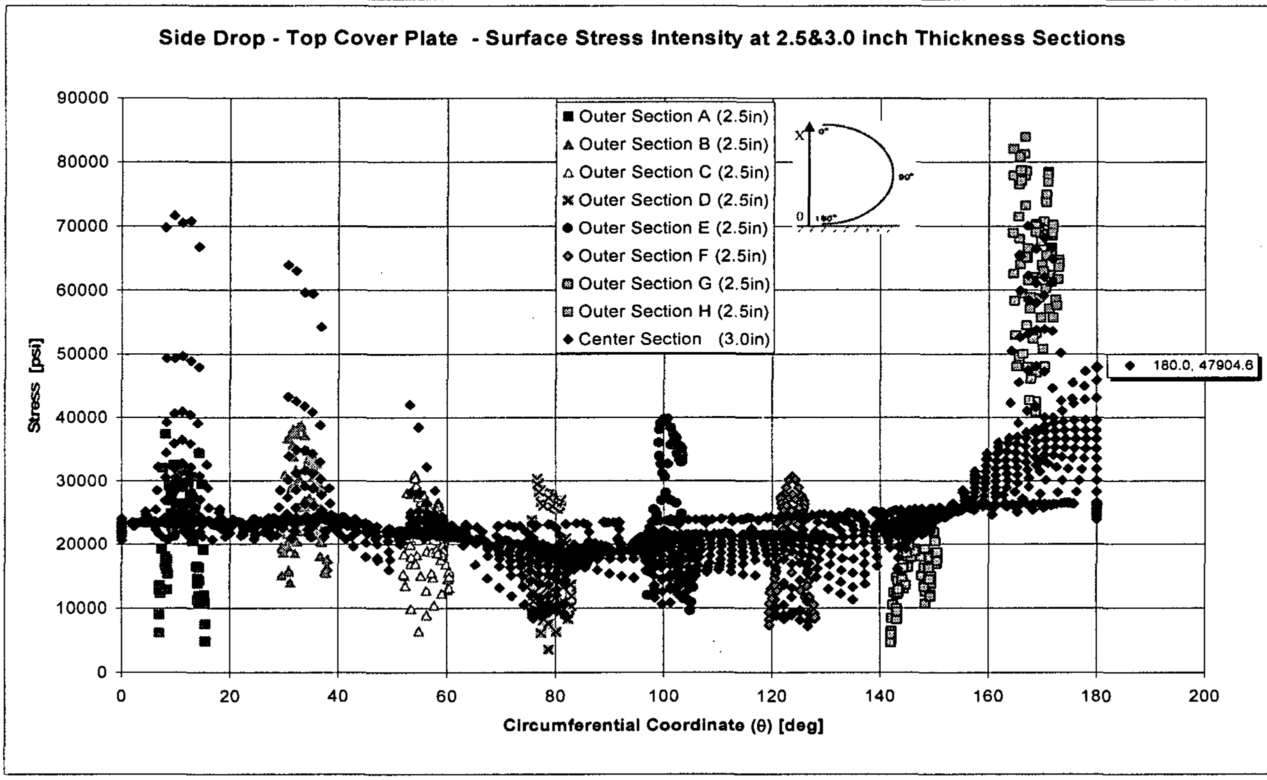

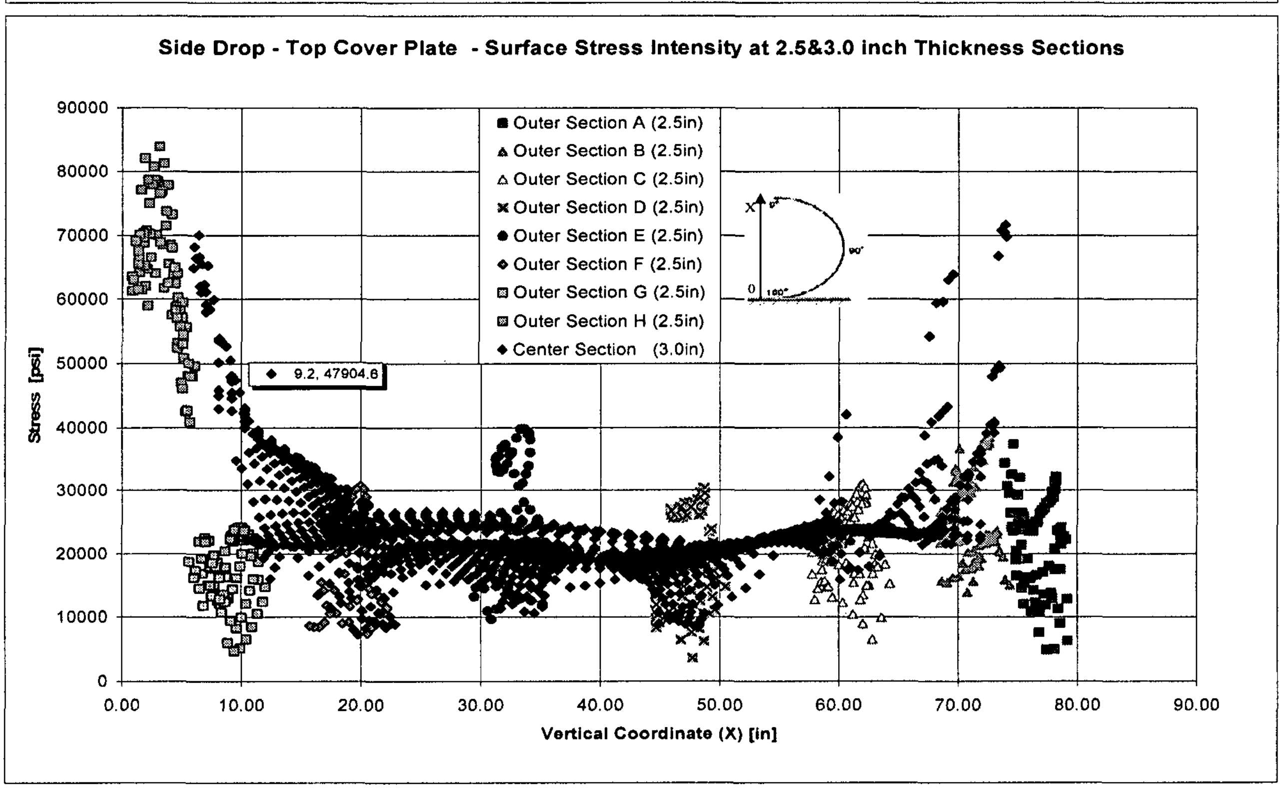

Figure 32 Top Cover Plate – Surface Stress Intensity at Predefined Sections

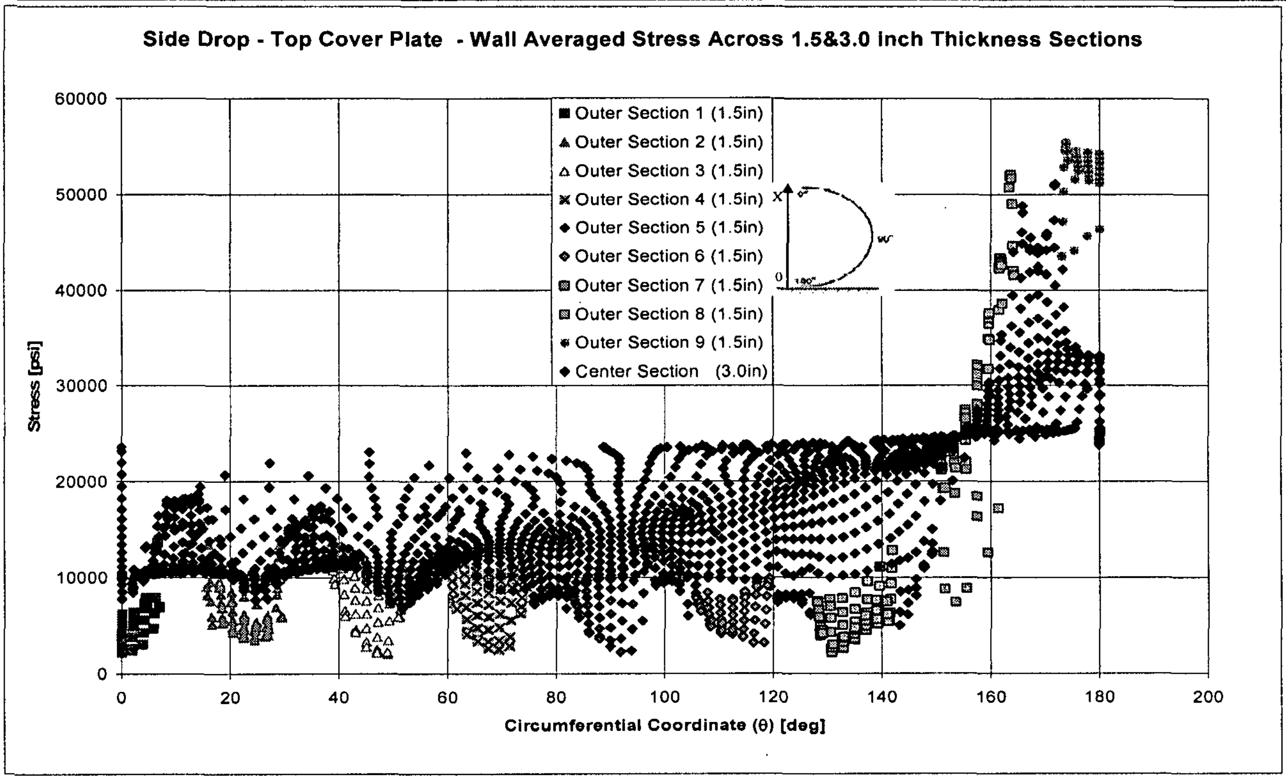

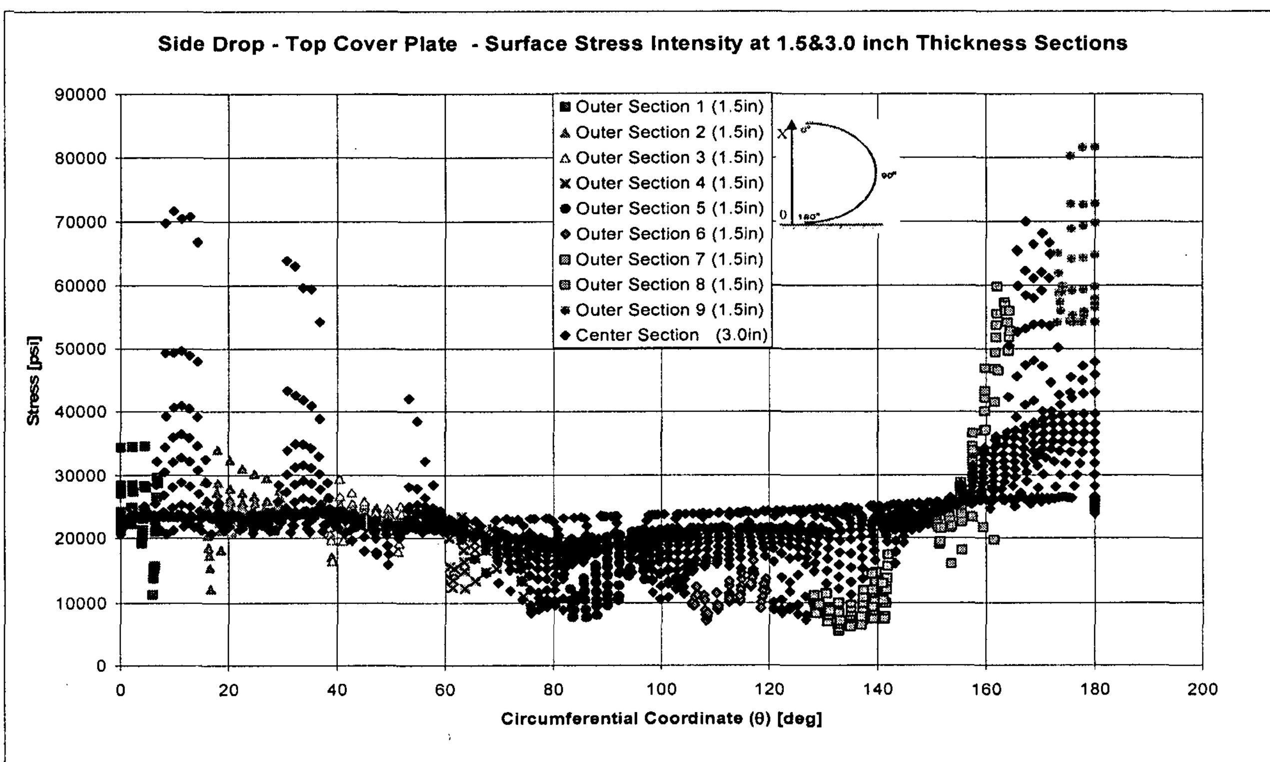

Figure 33 Top Cover Plate – Stress Intensity at Predefined Sections

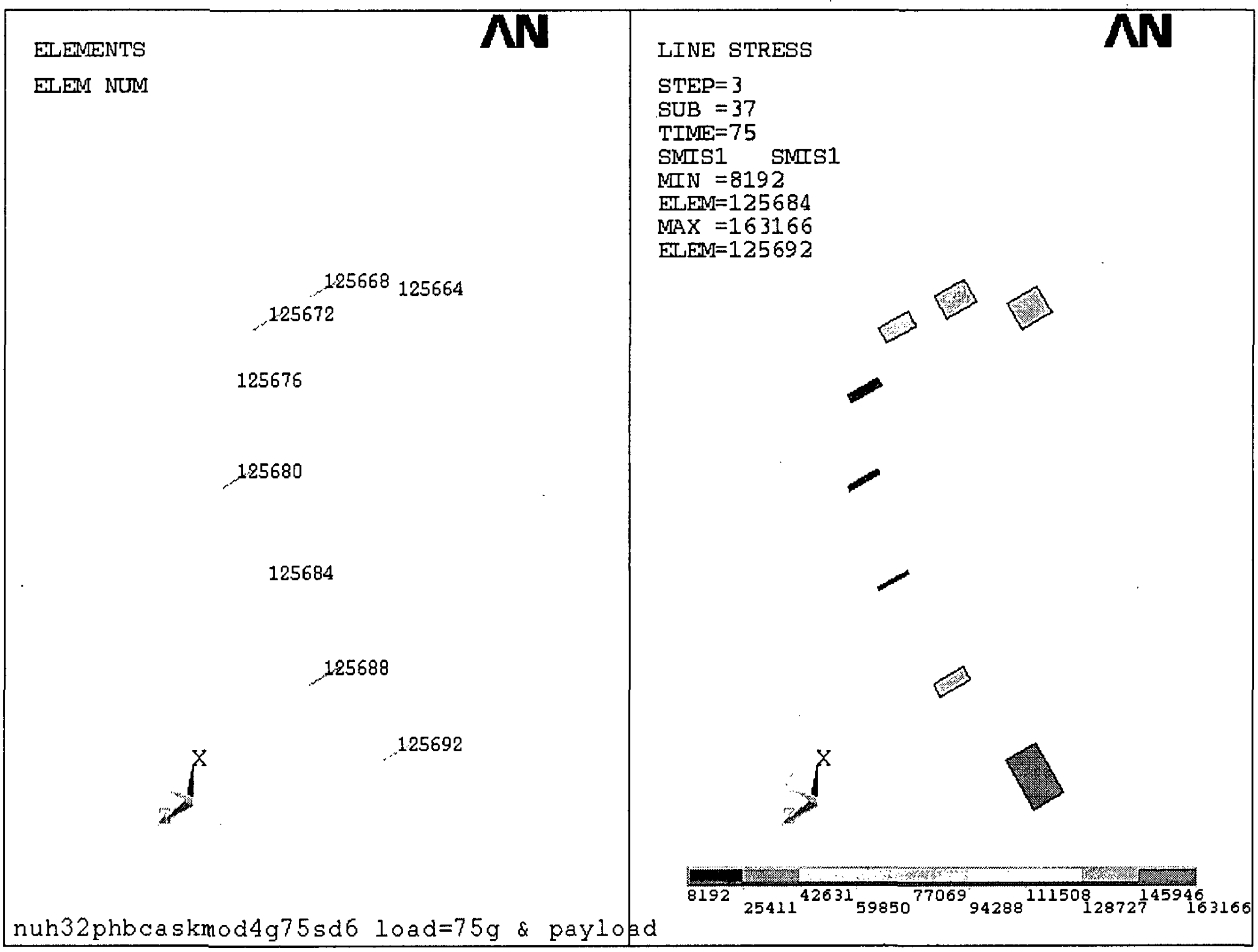

Figure 34 Top Cover Plate Bolts (left plot) – Bolts Tensile Force (right plot)